NASA Contractor Report No. 66167

DESIGN OF A SOFT X-RAY ABSORPTION-MODE GAS DENSITY MEASURING SYSTEM

By David B. Hakewessell

Prepared under Contract No. NAS1-5577 by

GIANNINI CONTROLS CORPORATION
Control/Nucleonics Division
Duarte, California

for

NATIONAL AERONAUTICS AND SPACE ADMINISTRATION

ABSTRACT

for

DESIGN OF A SOFT X-RAY

ABSORPTION-MODE GAS DENSITY

MEASURING SYSTEM

By David B. Hakewessell

A soft X-ray absorption-mode gas density measuring system has been developed which operates on the principle that the quantity of soft X-rays absorbed in a gas is a function of the gas density. System operating parameters have been selected which provide a measurement accuracy of ±5% of density over a range of 0.01 atmosphere to 1.0 atmosphere, with measurement path lengths of 2.5 to 61 cm. A prototype system has been assembled, calibrated, and tested and is ready for installation in gas-flow facilities needing this measurement capability.

TABLE OF CONTENTS

TABLE OF CONTENTS - Continued

DESIGN OF A SOFT X-RAY ABSORPTION-MODE GAS DENSITY MEASURING SYSTEM

By David B. Hakewessell

SUMMARY

A soft X-ray absorption-mode gas density measuring system has been designed, fabricated, and tested. The system operates on the principle that the quantity of soft X-rays absorbed in a gas is a function of the gas density. System test results are in agreement with theories relating absorption characteristics to gas density. Using these relationships, system operating parameters have been selected which provide a measurement accuracy of ±5% of density over a range of 0.01 atmosphere to 1.0 atmosphere with measurement path lengths of 2.5 to 61 cm.

Hardware has been assembled, calibrated, and tested which meets all of the stated requirements and is ready for installation in test facilities needing this measurement capability.

INTRODUCTION

The soft X-ray absorption-mode density measuring system was designed to provide a means for determining air densities of a flowing stream. The measurements are made using a technique that does not disturb the gas flow properties. The system is capable of measuring the average gas density over a wide range of measurement path lengths.

The purpose of the work reported in this document is to design, fabricate, test, and deliver an air density sensing system which uses the absorption of soft X-rays as the method of measurement. A highly collimated beam of X-rays is directed through the gas to be measured. The quantity of X-rays that reach a detector without being absorbed by the gas provides the measure of gas density.

The basic physics of the measurement is well known and understood. X-ray equipment of the type used has been available for many years in X-ray spectrometers. The system design stems from this equipment, thus allowing maximum use of proven hardware. Each element of the system has been selected to provide the best performance for each particular job. The assembly is fabricated into a unit shown in figure 1. In certain cases where the standard hardware configuration was not capable of meeting the required accuracy, special techniques were developed. For example, in some regions of operation the X-ray output flux must be stable and repeatable to within ±0.3%. To

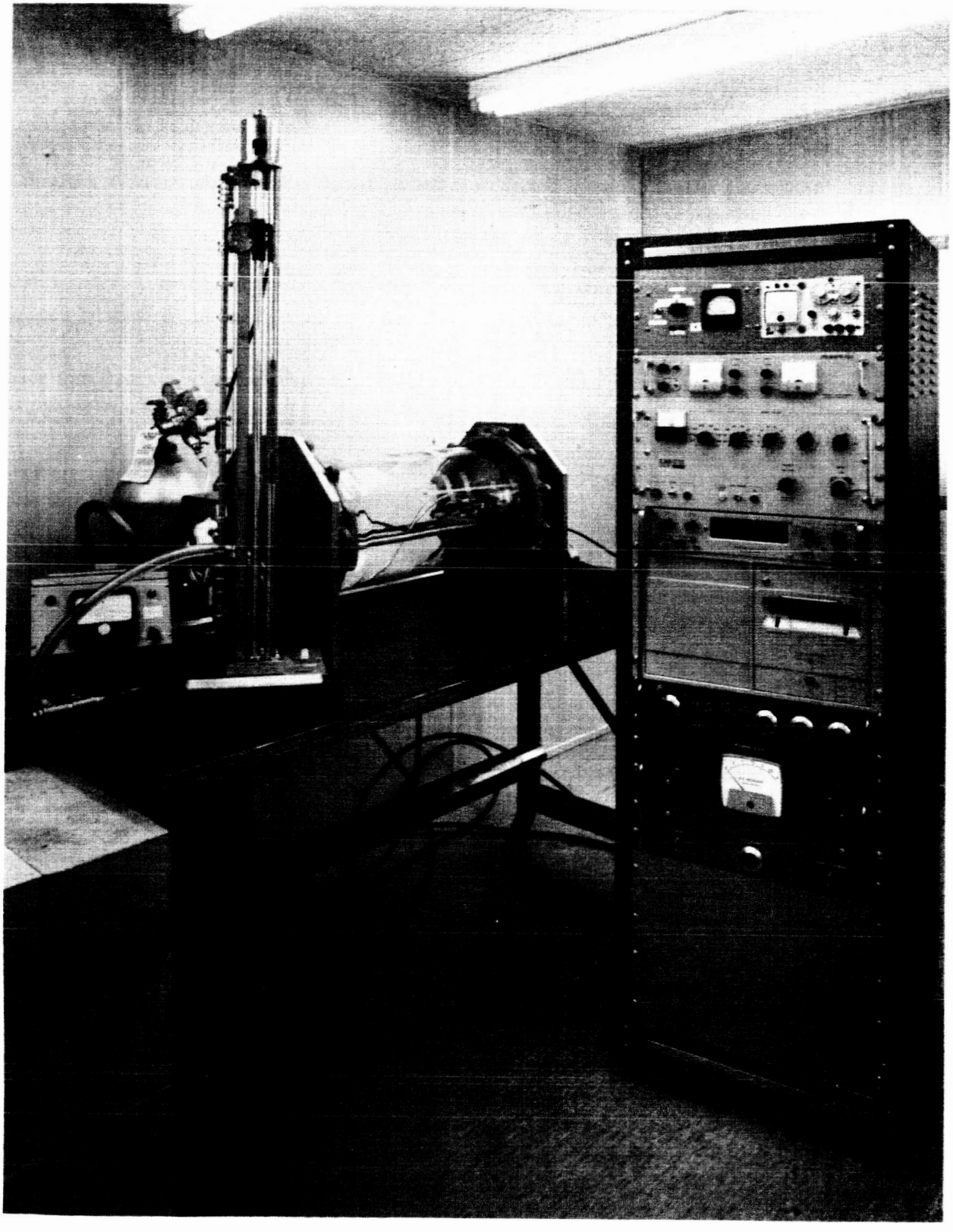

FIGURE 1 - Photograph of Soft X-ray Absorption Mode Gas Density Measuring System

meet this stringent requirement, a special output flux stabilizing system was designed.

Extensive performance testing of the system has been completed. A detailed error analysis has been performed and the important parameters experimentally verified. Results of these analyses and tests indicate that the system is capable of providing a gas density measurement over a 100:1 density range and a 61 cm to 2.5 cm path length with a measurement accuracy within ±5.0 percent of reading.

The interconnection and control logic of the system was designed to minimize accidental damage by providing overload protection and fail safe turn-on sequencing.

The significant contribution of this work is the verification of basic accuracy considerations, the successful modification of standard X-ray tubes to provide the necessary outputs, and the development of collimation techniques which provide the required beam widths.

The work reported in this document includes a listing of the overall system requirements, discussions of the theory of operation, a description of the hardware design, a theoretical analysis of the system performance, an experimental evaluation of system performance, instructions for system operation, a discussion of safety considerations, conclusions, recommendations, and applications.

SYMBOLS AND UNITS

The International Systems of Units will be used throughout this report.

The symbols used in this report are listed below.

D	Dose rate	rad/hour
E	X-ray energy	keV
G	Open loop transfer function	
I	X-ray intensity	Hz
I_b	Background pulse rate	Hz
I_d	Detected pulse rate	Hz
I_i	X-ray intensity at the anode	Hz
I_o	Initial X-ray intensity	Hz
I_t	True pulse rate	Hz
I_w	X-ray power	watts
i_p	X-ray tube plate current	milliamperes
K	gain	
K_1	Transfer characteristic of filament power supply	volts/volt
K_2	Transfer characteristic of X-ray tube	milliamperes/volt
K_3	Transfer characteristic of feedback resistor	volts/milliampere
K_a	Gain of preamplifier	
K_b	Gain of discriminator	
K_c	Gain of proportional counter	
n	Number of pulses	

SYMBOLS AND UNITS - Continued

P	Measured pressure	gm/cm^2
P_a	Air pressure	gm/cm^2
P_w	Partial pressure of water vapor	gm/cm^2
R	Gas constant	
R_a	Gas constant for air	
R_d	Feedback capacitor leakage resistance	ohms
R_f	Feedback resistance	ohms
R_i	Input resistance	ohms
R_w	Gas constant for water vapor	
S	Ratio of fractional gain change to fractional count rate change	
s	Laplace operator	
T	Gas temperature	°K
V_b	Discriminator base level setting	volts
V_c	Proportional counter excitation voltage	volts
V_f	Amplifier output voltage	volts
V_o	Amplifier offset voltage	volts
V_p	X-ray tube plate voltage	volts
V_r	Reference voltage	volts
x	Path length	cm
x_c	Thickness of counter gas	cm
x_w	Thickness of X-ray tube window	cm
Z	Atomic weight	
ϵ	Detector efficiency	
ϵ	Error signal	volts

SYMBOLS AND UNITS - Continued

ξ	Damping ratio	
μ	Mass absorption coefficient of air	cm^2/gm
μ_c	Mass absorption coefficient of counter gas	cm^2/gm
μ_w	Mass absorption coefficient of X-ray tube window	cm^2/gm
μ_w	Mass absorption coefficient of water	cm^2/gm
ρ	Gas density	gm/cm^3
ρ_a	Air density	gm/cm^3
ρ_c	Calibration density	gm/cm^3
ρ_c	Density of counter gas	gm/cm^3
ρ_w	Water vapor density	gm/cm^3
ρ_w	Density of X-ray tube window	gm/cm^3
τ	Detector resolving time	seconds
τ_1	Time constant of integrator	seconds
τ_2	Time constant of X-ray tube	seconds
ω_n	Natural frequency	radians/second

SYSTEM REQUIREMENTS

The objective of this work is to design and fabricate a soft X-ray absorption-mode gas density measuring system consisting of a highly collimated X-ray source, an X-ray detector, and associated electronic equipment. The system must provide an output which is a measure of the average gas density over the path traversed by the X-ray beam in air. The detail system

requirements are listed below.

1. Density Range - 0.01 atmosphere to 1.0 atmosphere
2. X-ray Beam Path Langth - Variable from 2.5 cm to 61 cm
3. X-ray Beam Diameter - Maximum beam diameter of 0.635 cm
4. Accuracy - Error less than ±5.0% of density
5. Response - Averaging time of one second
6. Safety - The X-ray source must be shielded in all directions save that of the beam to such an extent that no hazard will occur to operating personnel in the immediate vicinity of the source from spurious radiation.
7. End Use of Device - The device is for use in laboratory facilities for the measurement of gas density in and about hypersonic ramjet experimental engines.

THEORY OF OPERATION

This section presents the theoretical background pertaining to X-ray generation, absorption, and detection and how it applies to the problem of air density measurement. Figure 2 illustrates the basic system elements. X-rays are generated by the X-ray tube source. These X-rays are collimated into a narrow beam which is directed through the air volume where density is to be measured. In traversing the air volume, a portion of the X-rays is absorbed. The remaining flux is measured by the X-ray detector and compared with calibration data, thus providing the measure of density.

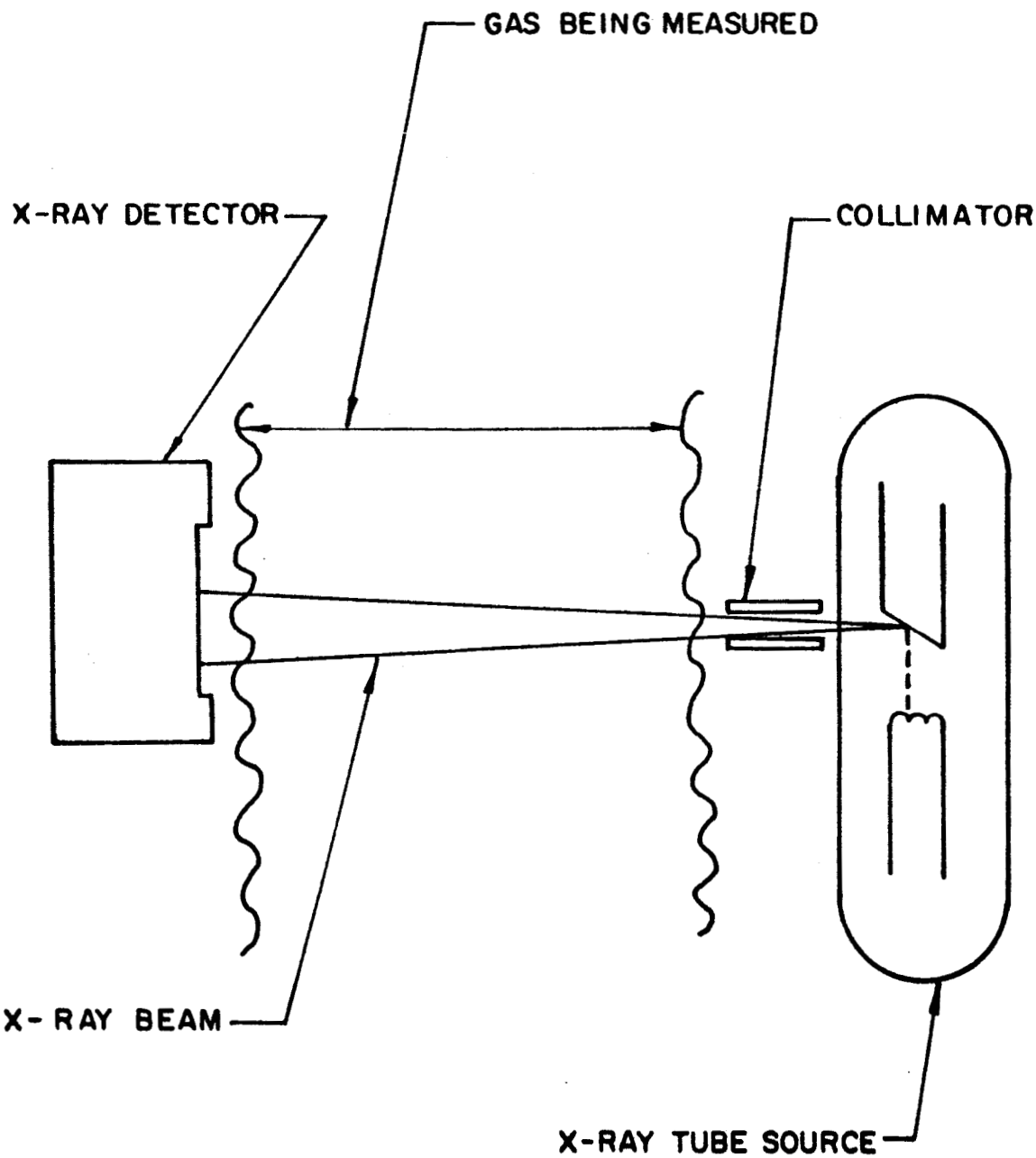

FIGURE 2 - System Elements and Geometry

Absorption Process

As the X-ray beam traverses the gas, a portion of the X-rays interacts with the gas. The interaction is either one of absorption or scattering for soft X-rays in the 1 to 5 keV energy range. As an X-ray is absorbed, its energy is transformed into energy of other types. Part goes into kinetic energy of ejected photo-electrons or recoil electrons, and part into potential energy of the excited atoms remaining. The moving photo-electrons and recoil electrons dissipate their energy in the gas by formation of ions. The excited states of the remaining atoms are in general short-lived, and as they return to a normal state, radiation is emitted which is absorbed in the parent atom or in adjacent atoms, with the ejection of electrons and subsequent loss of energy in the formation of ions. When an X-ray is scattered from the beam, it is eventually absorbed with its energy appearing as the energy of electron motion and subsequent ion formation.

In the absorption process the fraction $\frac{dI}{I}$, of the intensity, I, of the beam of X-rays absorbed as they pass through a thin layer of matter is proportional to the density of the material, ρ, and the thickness, dx, of this layer. Then

$$\frac{dI}{I} = -\mu\rho dx \qquad (1)$$

where μ is the factor of proportionality called the mass absorption coefficient. Integrating this expression through a distance, x, gives the expression

$$I = I_o e^{-\mu\rho x} \qquad (2)$$

where I_o is the initial beam intensity.

Knowing the initial intensity, I_o, mass absorption coefficient, μ, and path length, x, the detected intensity, I, gives the measure of density, ρ, as shown by

$$\rho = \frac{1}{\mu x} \ln \frac{I_o}{I} \qquad (3)$$

The mass absorption coefficient of air is a strong function of the X-ray energy as illustrated in figure 3. The X-ray energy is selected to provide the proper mass absorption coefficient, μ, for a particular distance, x, to obtain the desired scale factor.

The scattering coefficient for soft X-rays is 0.19 cm^2/gm (Ref. 1). This is a small portion of the mass absorption coefficient which ranges from 3,850 cm^2/gm to 37 cm^2/gm over the 1 to 5 keV X-ray energy range (Ref. figure 3). Scattering and dose buildup effects due to secondary scattering are thus neglected.

A portion of the atoms which are in an excited state as a result of an X-ray interaction regain their normal state by a process in which energy is liberated in the form of fluorescence X-ray. The energy of the fluorescence X-ray is determined by the atomic structure of the gas. The fluorescence energies resulting from electrons ejected from the K shell of oxygen and nitrogen are 0.532 keV and 0.400 keV, respectively. The ratio of fluorescence X-rays generated to electrons ejected is called the fluorescence yield and is a function of the atomic number. For low Z materials like oxygen and nitrogen, the fluorescence

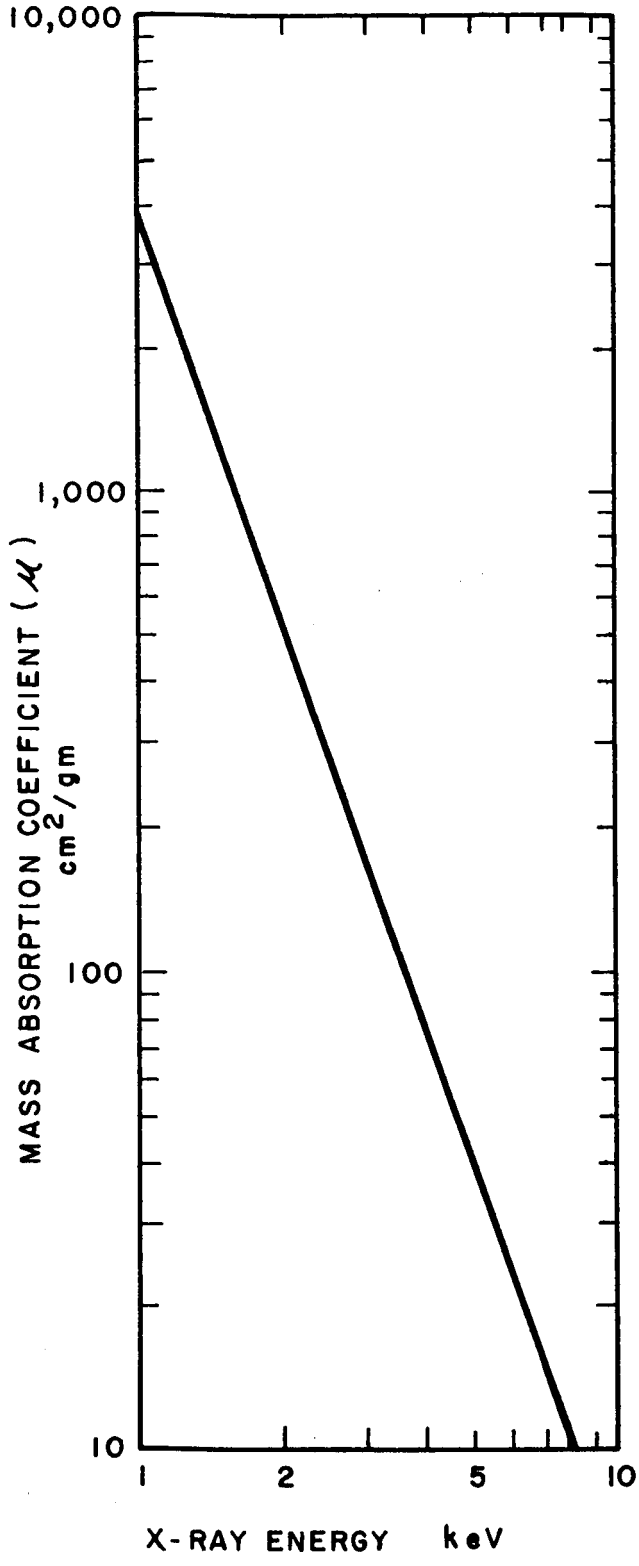

FIGURE 3 - Mass Absorption Coefficient of Air vs. X-ray Energy
(Computed from Constituent Data, Reference 2)

yield is very low, less than 0.01. Since each fluorescence X-ray may leave the atom in any direction, the portion that remains in the X-ray is small. These two factors indicate the fluorescence process contributes negligibly to the detected count rate.

From the above considerations the absorption process is seen to be purely exponential for a given X-ray energy. The resulting calibration curve is detected X-ray intensity versus density for a given energy and path length is illustrated in figure 4.

X-ray Source

The source of X-rays for the system is a conventional X-ray tube operating at 1,000 to 5,000 volt plate voltage and 0.2 to 10 milliamperes plate current. The generation of X-rays in an X-ray tube is accomplished by accelerating electrons through the plate potential toward a tungsten target. As these electrons hit the target they are decelerated rapidly with the resultant generation of bremsstrahlung radiation. A typical bremsstrahlung X-ray or continuous X-ray spectrum is illustrated in figure 5, curve 1. The upper energy limit is established by the accelerating potential. The decrease in intensity at low energy is the result of absorption of the softer X-ray component in the tungsten target.

The continuous X-ray spectrum is modified as the radiation passes out of the tube envelope through a thin beryllium window. This window absorbs a portion of the X-ray flux. The lower energy X-rays are absorbed to a larger extent than the higher

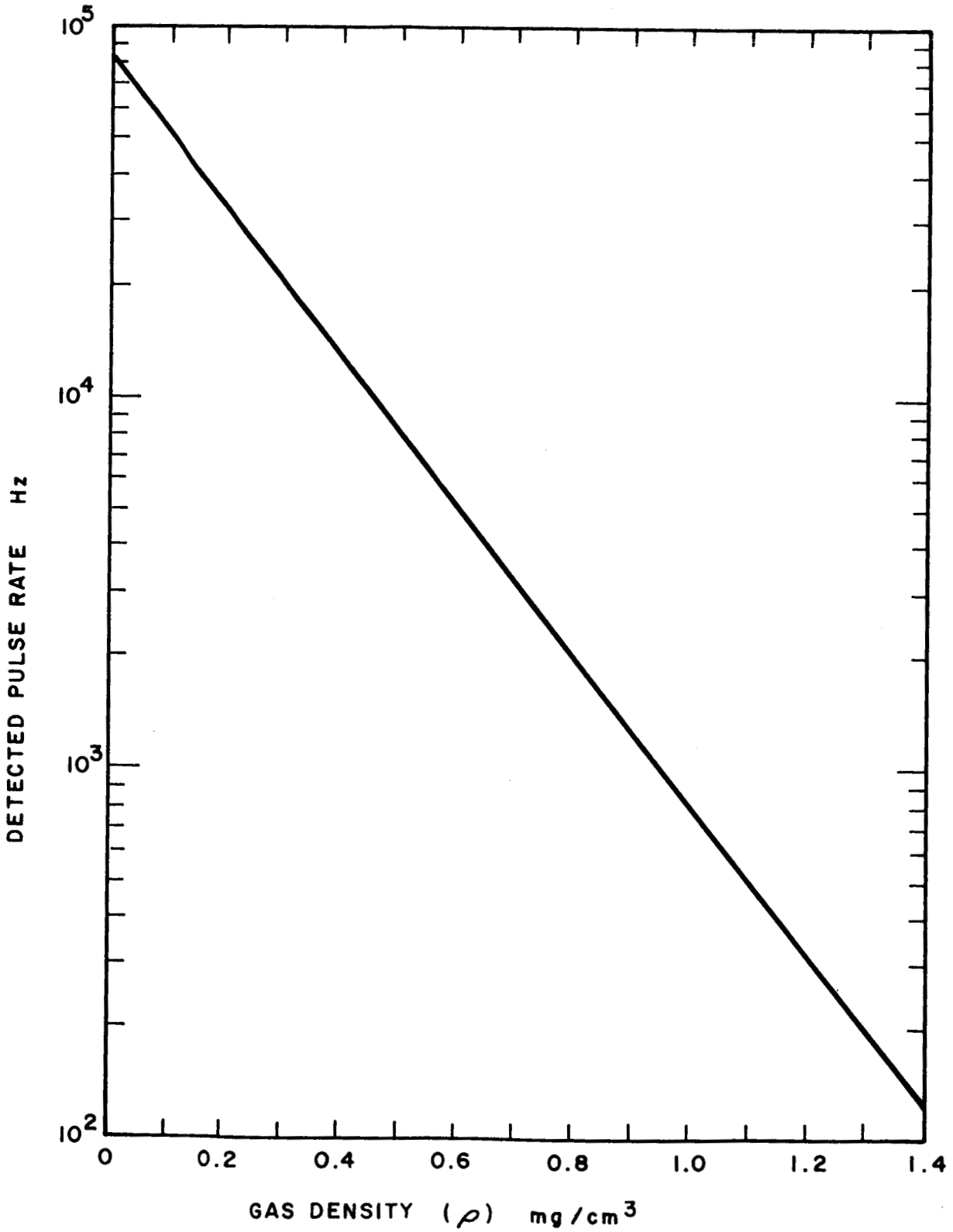

Figure 4 - Exponential Variation of Detected X-ray Intensity with Density

energy which modifies the spectrum, as shown in figure 5, curve 2. This preferential absorption results in a fairly narrow output spectrum whose energy is slightly below the plate voltage of the X-ray tube.

A second important X-ray generation mechanism results in an X-ray line, characteristic of the X-ray target material. In this mechanism electrons are ejected from the inner portion of atoms of the target material by the electron beam. When an electron returns to the vacated position, fluorescence X-rays are emitted. The fluorescence X-rays have discrete energies known as the K, L, and M characteristic radiations. The K line is most pronounced and the L and M lines less intense, respectively. For a tungsten target, these characteristic lines fall at approximately 69.5 keV, 12.1 keV, and 2.8 keV. The plate voltage of 1 to 5 keV is not high enough to excite the K and L lines and the intensity of the M line is negligible compared to the continuous spectrum. A copper target has characteristic lines at approximately 9.0 keV, 1.1 keV, and 0.14 keV. A fixed line at 1.1 keV has been noted in the X-ray tube tested, indicating the presence of a copper contaminant in the tungsten target.

The power of the continuous X-radiation is related to the plate current, plate voltage, and atomic number of the target material as in the following expression

$$I_w = 1.4 \times 10^{-12} \, i_p Z V_p^2 \qquad (4)$$

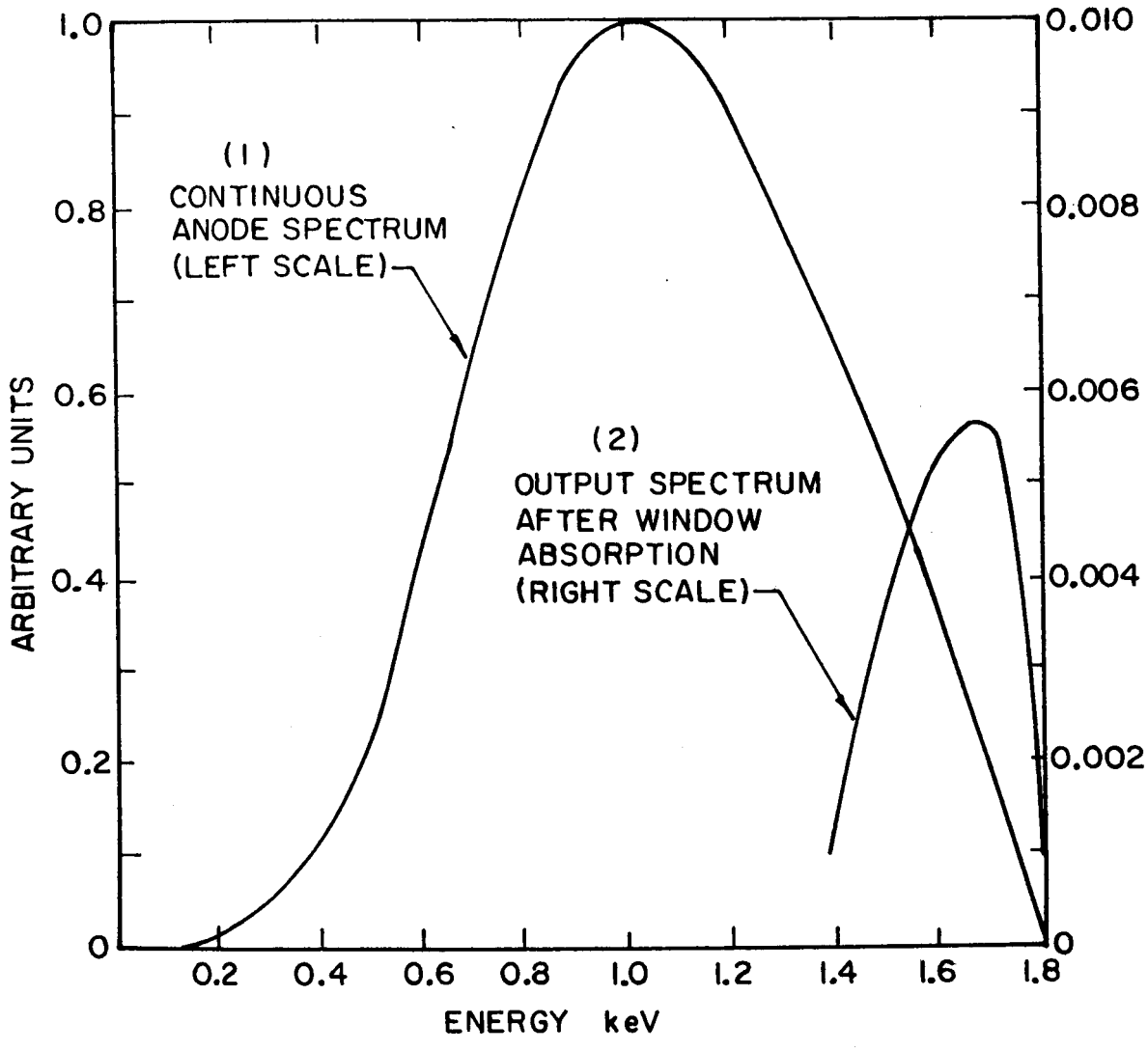

FIGURE 5 - X-ray Spectrum

where

I_w = output power in watts

I_p = plate current in milliamperes

Z = atomic number of target materials

V_p = cathode to plate voltage in volts

This shows direct proportionality of power to current and to the square of voltage. The X-ray output power is also a strong function of the attenuation in the beryllium window. The attenuation of the 0.0125 cm thick beryllium window as a function of X-ray energy is illustrated in figure 6. This shows a strong output sensitivity to X-ray energy at the lower energies, indicating the need of a highly stable plate voltage to maintain a stable output flux.

Collimator

The X-ray output must be collimated into a beam whose diameter does not exceed 0.635 cm over a 61 cm path length. Since the X-ray tube target spot is of finite dimensions, the X-ray tube cannot be considered a point source. This condition eliminates the possibility of using a single pin hole type collimator. Referring to figure 7a, it is seen that a collimator is required with a diameter to length ratio of 1:200. For the collimator to be reasonable length, 5 cm or less, the collimater diameter must be 0.025 cm or less. The collimator

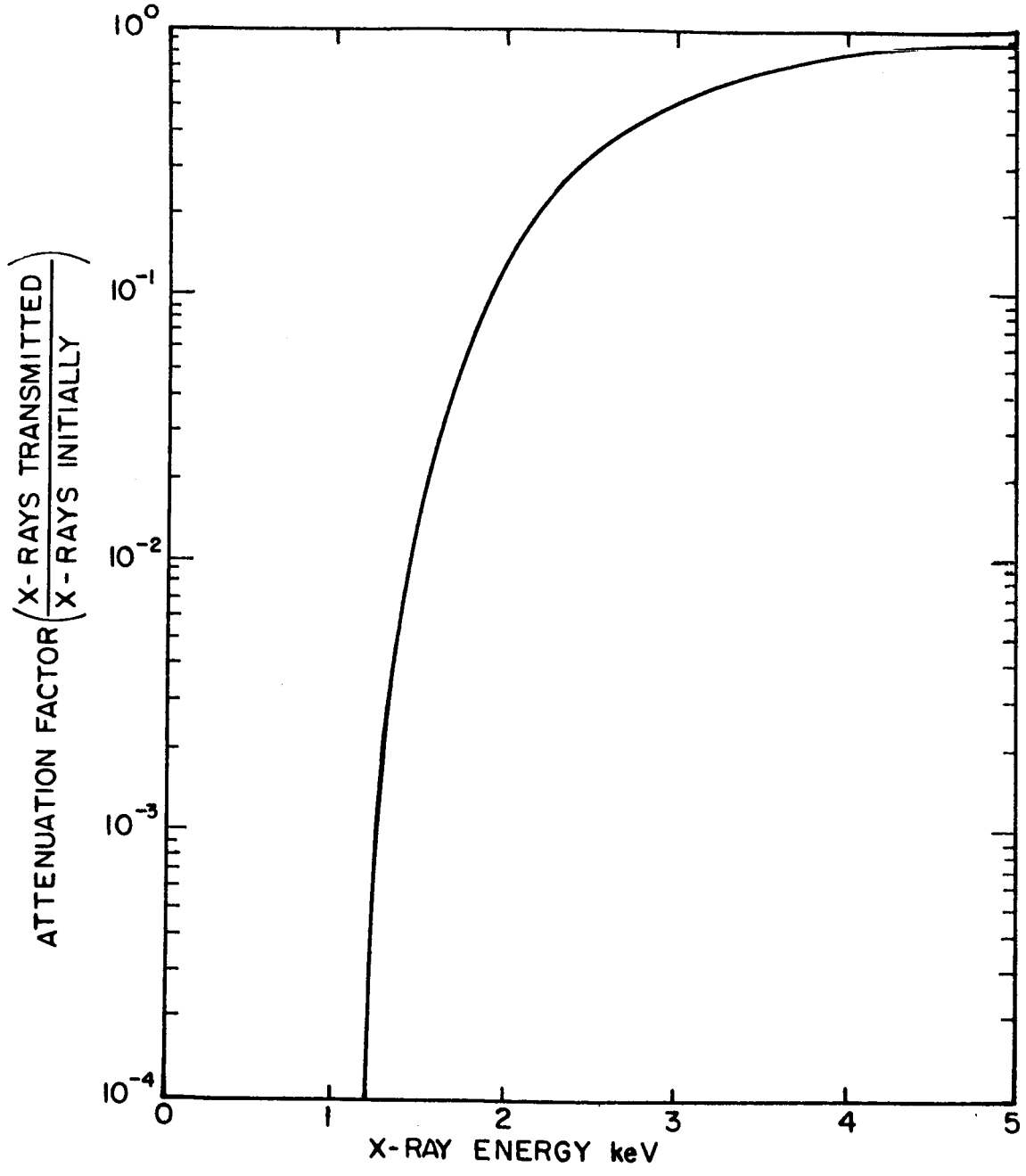

FIGURE 6 - X-ray Attenuation of a 0.0125 cm thick Beryllium Window

meeting this constraint was designed using a bundle of parallel hypodermic tubes. Each tube has a length of 5 cm or less and an inside diameter of the required 0.025 cm. The tube bundle is 0.635 cm in diameter. The resultant intensity profile calculated by summing the theoretical profile of each tube is shown in figure 7b. At the 61 cm distance, 80 percent of the flux falls within a 0.635 cm diameter circle.

For the shorter path lengths, the collimation requirement is not as stringent and so shorter length collimators are used. For example, a 0.635 cm long collimator with 0.025 cm ID tubes provides a beam width of 0.635 cm at a distance of 6.5 cm. The collimator lengths selected for the various measurement distance ranges are given below.

Collimator Length (cm)	Measurement Path Length (cm)
5.0	25.0 - 61.0
2.5	12.5 - 25.0
1.25	5.0 - 12.5
0.635	2.5 - 5.0

Detection

A proportional counter detector was chosen over other types, such as solid state and scintillator/photo tube detectors, because it exhibits the lowest noise and highest resolution in the 1-5 keV energy range. The proportional counter chosen is 3.34 cm diameter by 11.45 cm long. The counting gas is 90% argon and 10% methane. The window material is 0.00038 cm thick mylar. As the X-rays

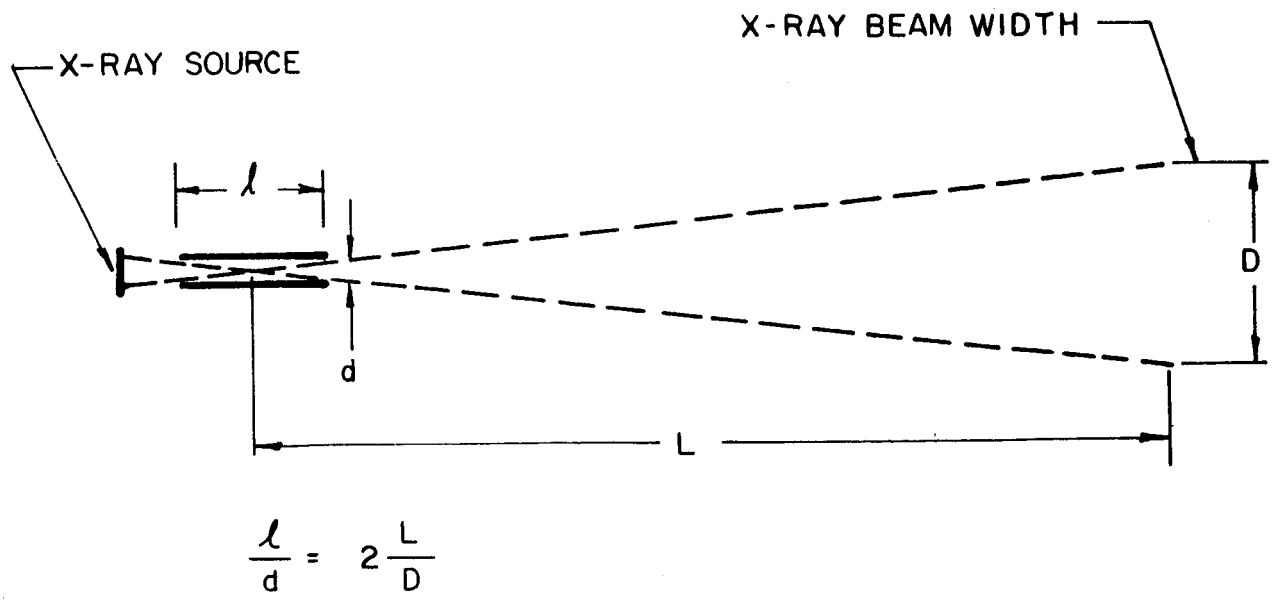

$$\frac{l}{d} = 2\frac{L}{D}$$

FIGURE 7a

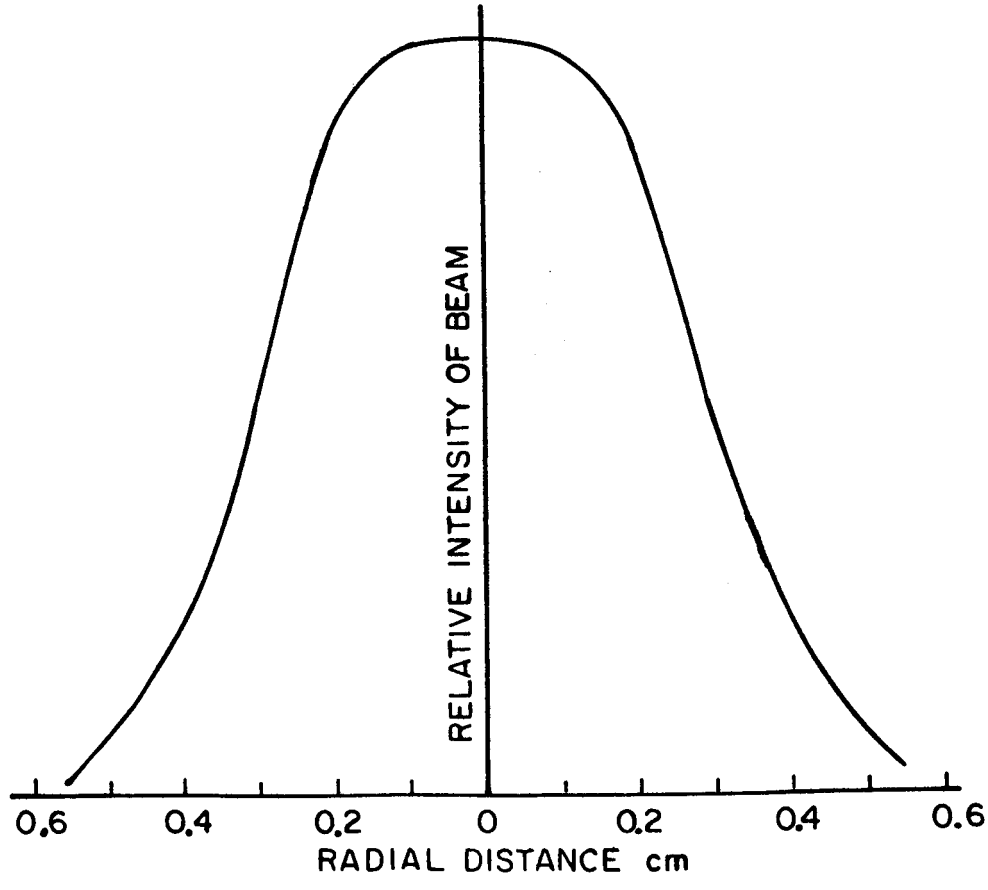

FIGURE 7b - Collimator Characteristics

enter the proportional counter, they interact with the gas forming ions. A voltage potential applied across the counting chamber accelerates these ions to energy sufficient to ionize further the gas molecules by collision. The higher the potential, the greater will be the energy of the secondary ions formed, and the greater the total ionization produced. A "gas amplification factor" is thus introduced which increases with voltage. The proportional counter is operated at a voltage such that the total ionization formed is proportional to the energy lost to the gas by the X-ray particle. The electrons are collected at the anode, creating a voltage pulse whose amplitude is proportional to the X-ray energy.

The rise time of the voltage pulse is rapid since the electrons are quickly drawn to the anode. The decay time is much slower, representing the time required for the heavier positive ions to reach the cathode. The rise times are typically 0.5 μ second and decay times 5.0 μ seconds.

The efficiency of the counter tube is a function of the energy of the X-ray. Very high energy X-rays have a high probability of passing through the counter gas with no interaction and thus the efficiency is low. Very low energy X-rays have a high probability of being absorbed in the counter tube window and thus the efficiency is low. Figure 8 shows the percent efficiency versus X-ray energy for the counter tube showing a peak efficiency at 3.5 keV of 93%. The break in the curve at 3.2 keV is at the K edge of the argon gas.

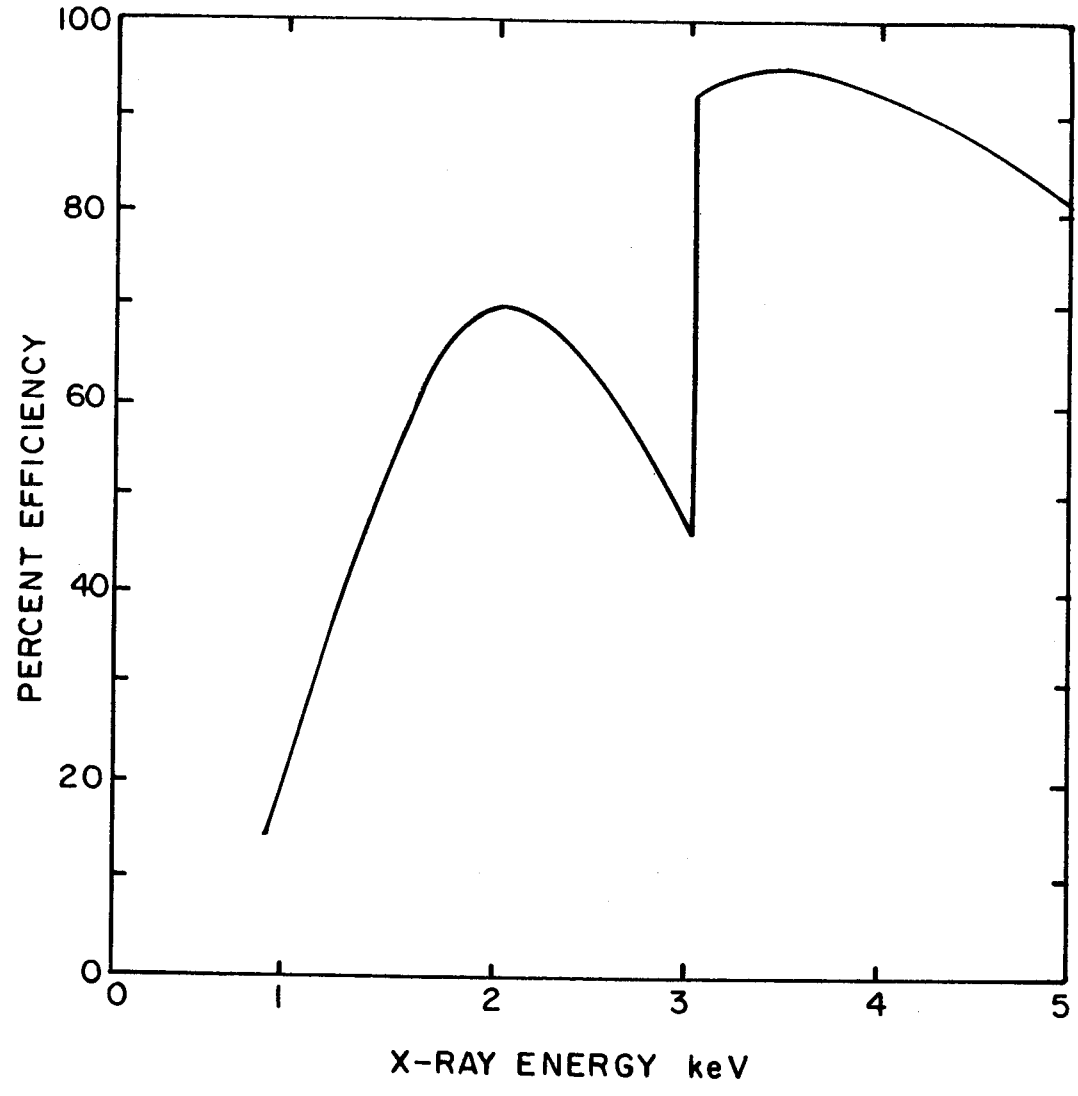

FIGURE 8 - Detector Efficiency

The range of counting rates required of the counter is 200 Hz to 80,000 Hz. The resolution time of the counter is hampered by the long output pulse decay. To improve the counter resolution, the counter output is fed immediately to a differentiation circuit. This provides a pulse whose amplitude is still proportional to the counter output but whose width is less than 1 μ second. The inability to resolve pulses less than 1 μ second apart causes count losses at the high count rates due to the random nature of the counting events. The actual counting rates are related to the input flux by

$$I_d = \frac{I_t}{1 + I_t \tau} \qquad (5)$$

where I_t is the true rate of arrival of events, I_d is the measured rate of arrival of events, and τ is the resolution time.

At extremely high counting rates there is a positive ion sheath buildup around the anode due to the relatively slow transport time for the positive ions to reach the cathode. This positive ion sheath changes the potential gradients near the anode which results in a reduction in gas amplification. The output pulse heights thus decrease as the counting rates reach high values.

A typical pulse height spectrum obtained with the proportional counter is shown in figure 9. The gamma rays counted are at 5.9 keV from an Fe-55 radioisotope source. The proportional counter is seen to have a pulse height resolution capability of about 30% at 5.9 keV (spectrum width at half amplitude). An

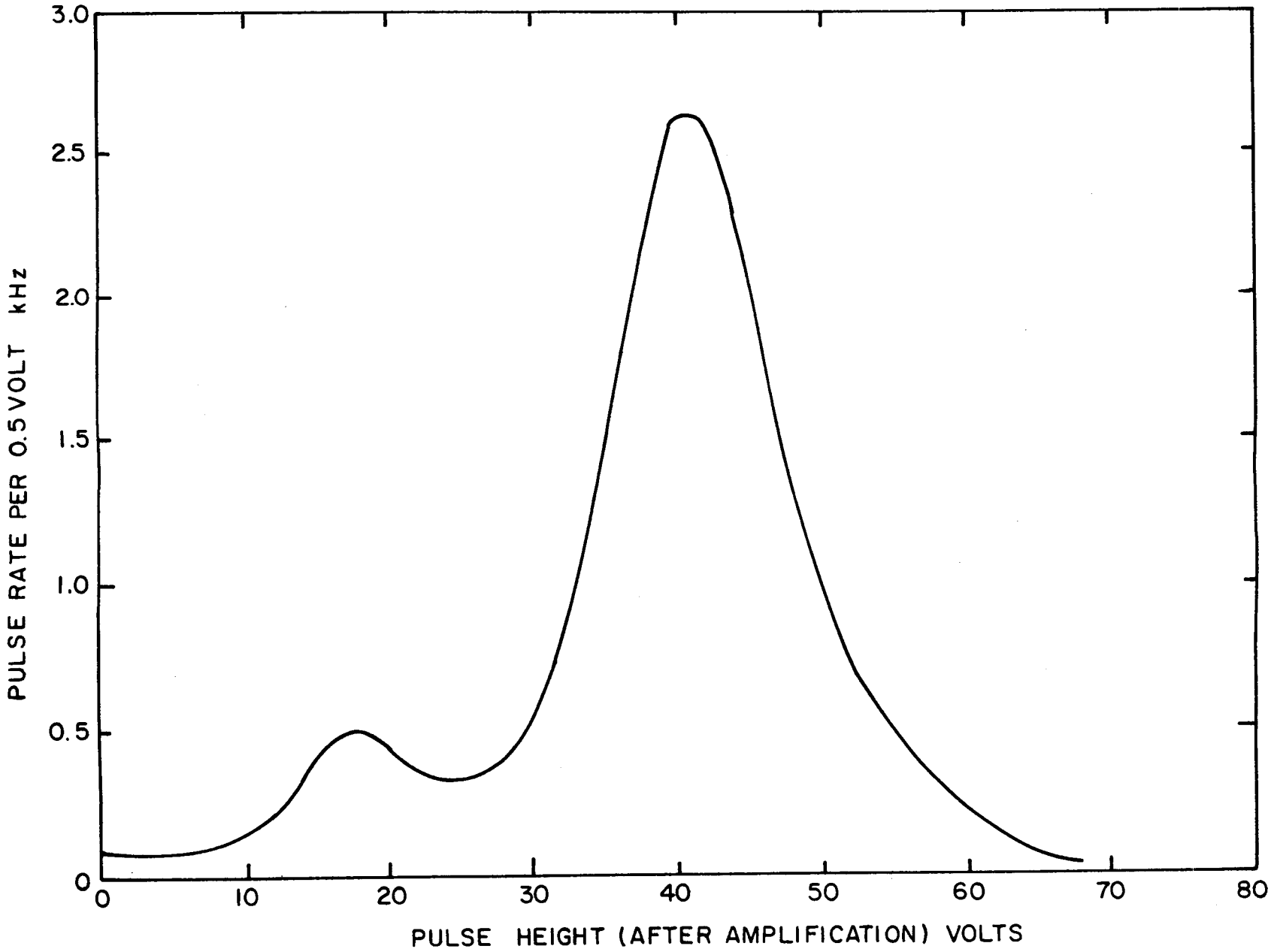

FIGURE 9 - Pulse Height Spectrum of 5.9 keV Fe-55 Gamma Measured with the Proportional Counter

X-ray spectrum is shown in figure 10, measured at three counting rates. A shift in counter gain is evident. The effect of this gain variation is minimized by counting all pulses above a given threshold voltage level. This level is set high enough to reject noise and low enough such that shifts in gain do not significantly affect the total count rate. The background levels with such a setting are very low, typically less than 2 pulses per second.

The counter gain is a function of the high voltage applied from anode to cathode. Using the single low level pulse height discriminator minimizes effect of gain variations due to high voltage variations.

HARDWARE DESCRIPTION

This section describes the hardware configuration of the gas density measurement system. The pertinent specifications for the system elements shown in the block diagram of figure 11 are given and the various modes of system operation are discussed.

General Description

The heart of the system shown in figure 11 is a conventional X-ray tube modified for low voltage operation with a 0.0125 cm thick beryllium window. The X-ray tube plate voltage is supplied by a 0-10 kV highly regulated power supply. Filament current is supplied by a regulated power supply. The X-ray tube anode current passes through a 100 ohm resistor and the voltage thus developed is compared to a reference voltage by the plate current

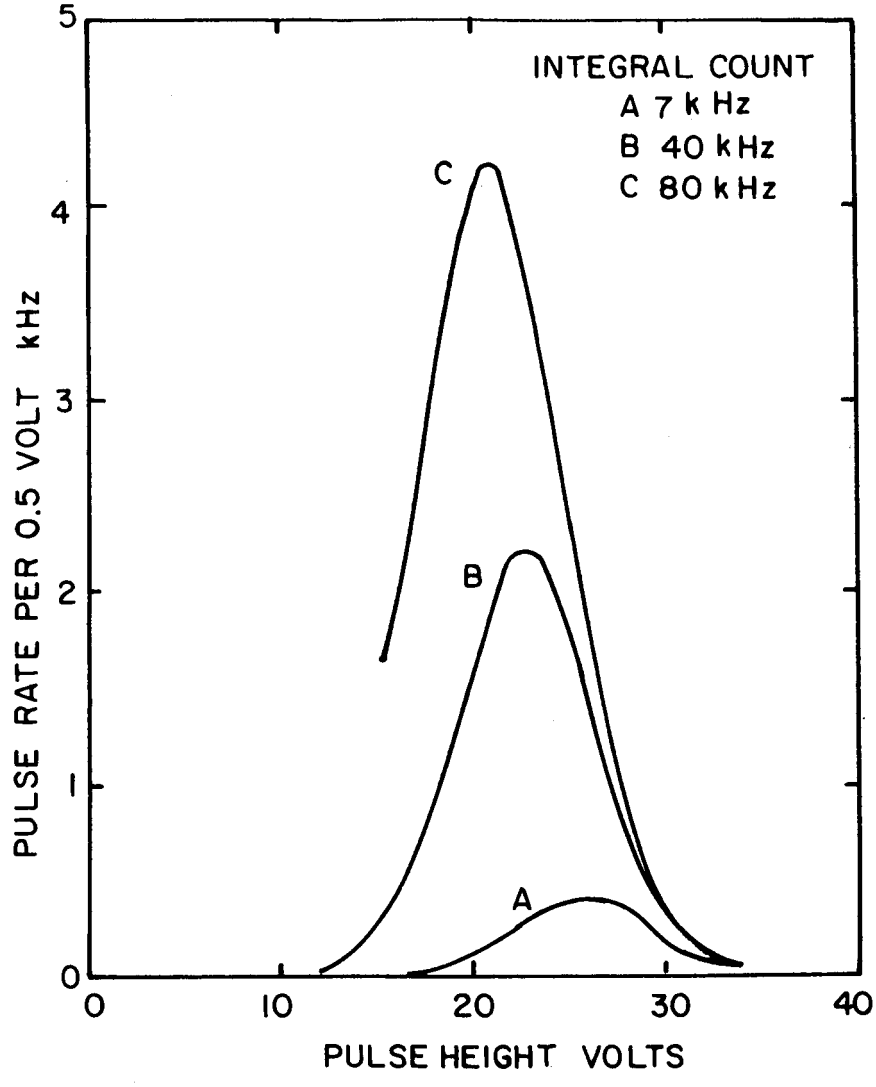

FIGURE 10 - Pulse Height Spectrum Showing Gain Shift with Count Rate

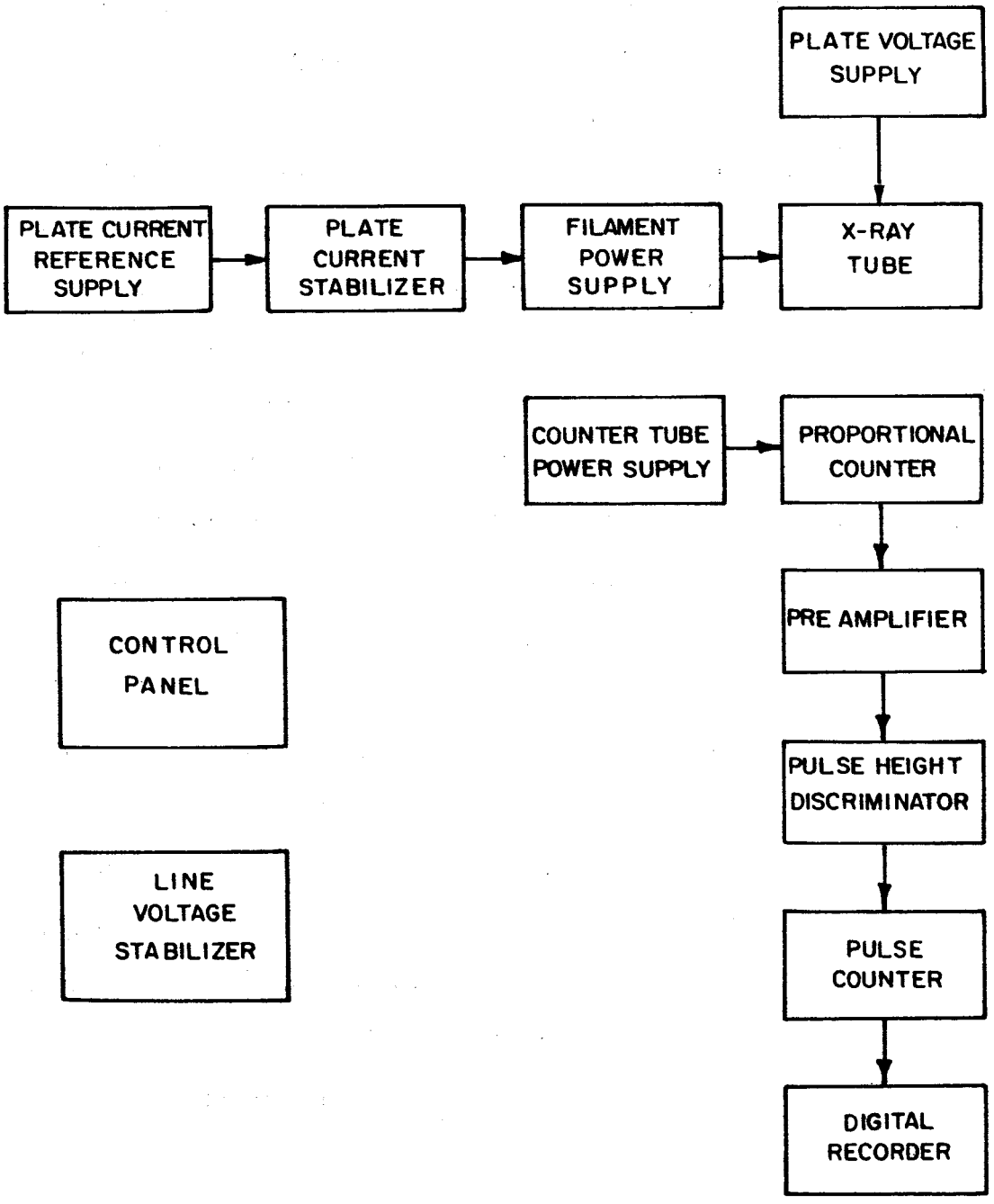

FIGURE 11 - System Block Diagram

stabilizer. The output of the plate current stabilizer is fed to the programming terminal of the filament power supply and is used to correct variations in anode current by adjusting filament temperature. The reference voltage is supplied by a precision reference voltage supply.

The detection portion of the system is comprised of elements of an X-ray Spectrometer. The X-ray detector is a proportional counter tube filled with a 90% argon 10% methane gas. The proportional counter is driven by a high voltage power supply nominally set for 1650 volts. The output of the proportional counter tube is amplified by the preamplifier. This amplified signal is then further amplified and operated on by a pulse height discriminator. The output of the pulse height discriminator drives a pulse counter, which in turn drives a digital recorder.

The control panel selects the various basic modes of system operation by means of a five position rotary switch. This panel also provides mounting for the X-ray tube plate current stabilizer and automatic reset and overload sensing circuitry. The line voltage stabilizer provides stabilized power to the system.

Component Parameters and Functions

Important component parameters and functions are described in this section.

X-ray Tube. - The X-ray tube has the following characteristics:

Minimum plate voltage:	1 kV
Maximum plate voltage:	20 kV

Maximum filament current	2.05 amperes
Maximum continuous plate current:	10 mA
Minimum window diameter:	0.625 cm
Maximum window thickness:	0.0125 cm
Filament life at maximum ratings:	1000 hours

The anode is cooled by forced air to allow continuous operation at maximum ratings.

X-ray Tube Plate Voltage Supply. - The plate voltage supply has the following important characteristics:

Output voltage:	0 to ±10,000 Vdc
Output current:	0 to 15 milliamperes
Line regulation:	0.001% or 2 mV (whichever is greater) for 10% line change from nominal
Load regulation:	0.001% or 5 mV (whichever is greater) for full load change
Stability:	±0.005% per hour; ±0.02% per day after warmup
Calibration accuracy:	±0.25% or 250 mV (whichever is greater)
Resetability:	±0.05% or 50 mV (whichever is greater)
Temperature coefficient of output:	Less than 20 parts per million per °C from +10°C to +40°C

Overload protection: HV turned off if plate current exceeds 13 mA

Filament Power Supply. - The filament power supply has the following important characteristics:

Output voltage: 0-36 Vdc

Output current: 0-5 amperes

Remote Voltage Program Capability

Plate Current Stabilizer. - The plate current stabilizer is an integrating operational amplifier which supplies the program voltage to the filament power supply. The operational amplifier has its own power supply. This stabilizer has the following important characteristics:

Feedback resistor temperature sensitivity: 250 ppm per °C

Input resistor temperature sensitivity: 250 ppm per °C

Feedback capacitor leakage resistance: >1000 megohms

Amplifier offset voltage drift: 50 μV per day

Amplifier offset temperature sensitivity: 0.6 mV per 10°C

Plate Current Reference Supply. - The plate current reference supply has the following important characteristics:

Output voltage: 0-20 Vdc

Output current: 0-500 milliamperes

Line regulation: 100 μV for 10% line variation

Load regulation: 100 μV for 100% change in rated load

Stability: Less than 0.001% plus 100 μV drift per eight hours

Temperature Coefficient: 0.005% or 30 μV, whichever is greater, per degree centigrade

Resolution: 10 μV

Proportional Counter Tube. - The proportional counter tube has the following important characteristics:

Dimensions: 3.34 cm diameter, 11.45 cm long

Operating voltage: 1400-2000 volts

Gas: Argon 90%, Methane 10%, continuously flowing with pressure slightly above atmospheric

Path Length: 2.5 cm

Window: Mylar, 0.00038 cm thick, 1.43 cm wide, 2.22 cm high

Counter Tube Power Supply. - The counter tube power supply provides voltage to the counter tube plus several voltages used in the detection system. The power supply has the following important characteristics:

High voltage output: 500-3000 Vdc (System operates at 1650 Vdc) (Pot setting 0.730)

HV repeatability 0.03%

HV line regulation: 0.005% for 1% variation of input voltage

HV drift: +0.03% for first 1/2 hour of operation

HV temperature stability: -0.035% for an increase of 10°C from a nominal operating temperature

Low voltage outputs: +250 Vdc at 200 mA
6.3 Vac at 3 amperes
-105 Vdc at 10 mA

Preamplifier. - The preamplifier has the following important characteristics:

Gain: 1.0

Gain stability: ±0.5% for a line voltage variation of ±1% input to the power supply

Temperature sensitivity: 0.1% for 5°C temperature variation

Pulse Height Discriminator. - The pulse height discriminator amplifies the pulses from the preamplifier and then rejects all pulses below the base level setting. This component has the following important characteristics when set up to operate in the soft X-ray gas density measurement system.

Amplifier gain variable: 20 to 500
(System coarse gain switch setting: 16)
(System fine gain potentiometer setting: 0.875)

Input pulse height: 0-16 millivolts

Pulse height selector amplitude range: 1.0-100 volts

Amplifier gain stability: ±0.3% for a line voltage variation of ±1% input to the power supply

Amplifier gain temperature sensitivity: 0.1% for 5°C temperature variation

Amplifier gain drift:	0.1% for any 8-hour period
Pulse resolution	0.25 microsecond
Base line adjustment range:	0-100 volts
(System baseline potentiometer setting: 0.010)	
Base line stability:	±0.1 volt for ±1% variation of input line voltage
Base line temperature sensitivity:	0.3 volt for a 5°C increase in temperature
Base line drift:	+0.3 volt for first 1/2 hour operation; ±0.2 volt for any 8-hour period after warmup

Pulse Counter. - The pulse counter has the following important characteristics:

Frequency range:	0 to >2 MHz
Total pulse count:	0-999,000 pulses
Accuracy:	±1 count ±time base accuracy
Time base accuracy:	±2 parts in 10^6
Time gate:	10 μ seconds to 10 seconds (System set for 1 second)
Trigger level:	-100 to +100 volts, adjustable (System set for +1.5 volts dc)

Digital Recorder. - The digital recorder has the following important characteristics:

Accuracy:	Same as pulse counter
Printing rate:	5 lines per second, maximum
Column capacity:	6 columns

Control Panel. - The control panel provides switching and overload circuitry for operating the X-ray tube. A circuit diagram of the control panel is shown in figure 12. The modes of operation as selected by the position of the rotary switch are:

1. Normal

   In this position the filament power supply is connected for manual control of the filament voltage and current.

2. Zero Offset

   This position provides the operator with a means of accurately setting the amplifier offset voltage to zero. Offset voltage should be checked frequently and adjusted to within ±0.005 volt, as the repeatability of the system is affected by drifts in this parameter.

3. Off

   This position removes filament voltage and disables the system.

4. Filament Warmup

   This position provides a minimum of 30 seconds for the X-ray tube filaments to warm up at a reduced filament current before the plate voltage supply is enabled. After this warmup period, the plate voltage supply standby light comes on and the high voltage may be turned on.

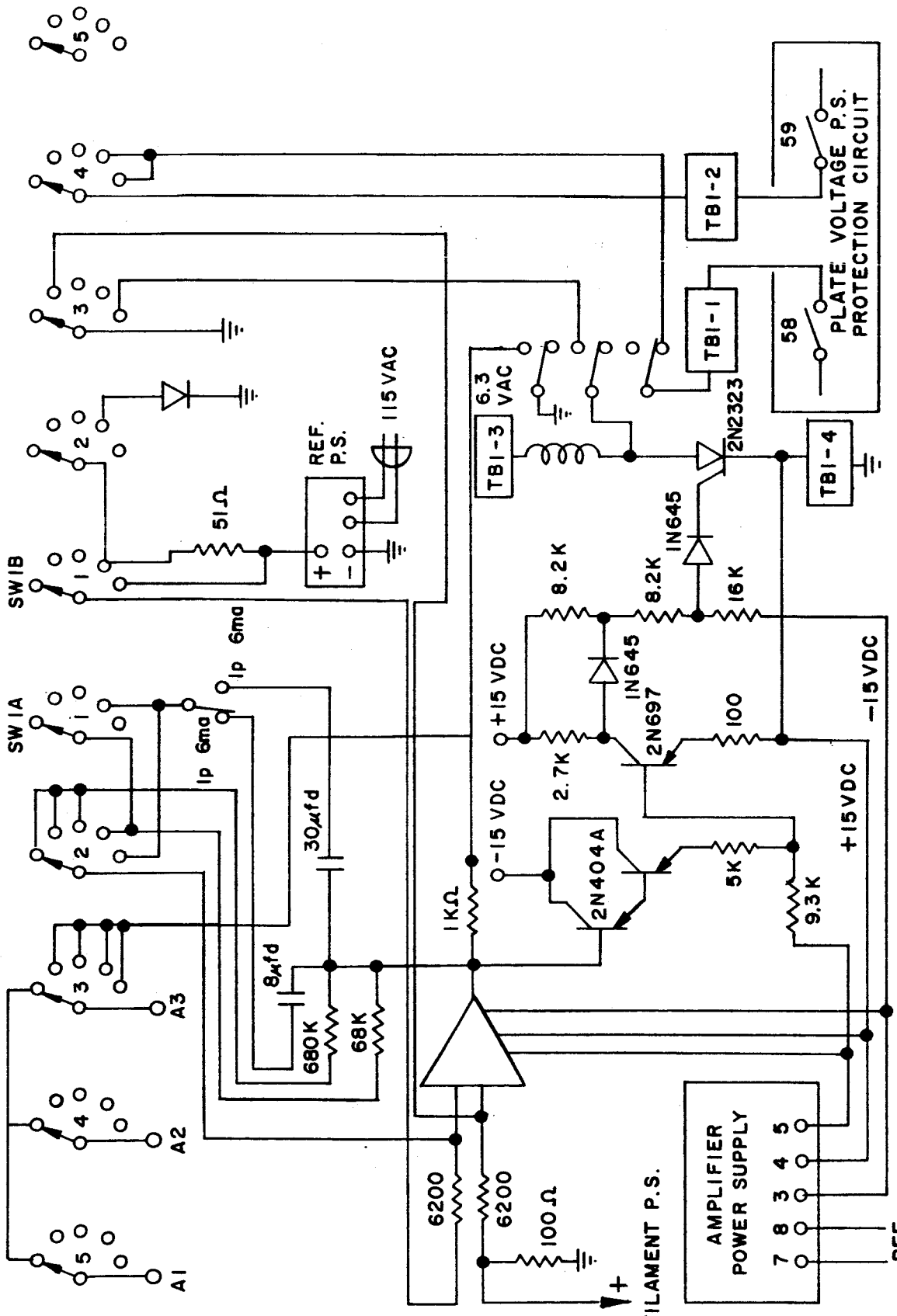

FIGURE 12 - Circuit Diagram of Control Panel

This filament warmup position forces the operator to turn the plate voltage supply standby/operate switch to STANDBY and wait for approximately 30 seconds until the standby light turns on. If for any reason the user switches to another mode of operation or does not place the standby/operate switch in standby, the plate voltage supply will not be enabled.

5. Operate

The operate position allows normal servo action to take place which controls the X-ray tube plate current at that value determined by the reference voltage setting. The normal range of plate current is zero to approximately 10 mA.

If an accidental overload occurs, the overcurrent protection circuit turns the plate voltage supply off and this event is sensed by the reset circuitry on the control panel. The reset circuitry removes voltage from the X-ray tube filaments and requires the operator to return to position 4 and to place the standby/operate switch in the standby position. Thirty seconds will be required after this sequence of operations for the plate voltage supply to recover. After the standby lamp has turned on, the plate voltage may again be turned on and the operation mode switch may be returned to position 5. If operation above 2.5 kV plate voltage is desired, it is

necessary to switch from standby to operate with the plate voltage set at below 2.0 kV to prevent a transient overload condition. Then while the mode switch is still in position 4 and the high voltage on, the high voltage may be switched from this nominal value up to the desired value.

If this procedure is not followed, the voltage transient resulting from the high voltage turn-on will actuate the reset circuitry and once more disable the system.

The system loop gain varies in a non-linear manner as a function of plate current. It was therefore found necessary to provide two time constants for the system feedback amplifier; one time constant is for operation of the system at plate current below 5 mA and the other is for operation above 5 mA. The time constant switch is turned to the proper position prior to each operation. An improper time constant may cause the system to overload, thus actuating the reset circuitry, disabling the system.

A meter indicating the approximate value of the plate current is mounted on the control panel as a visual check of system operation.

The filament voltage overload circuit senses the program voltage input to the filament power supply. If this voltage is excessive (equivalent to filament current of greater than 2.05 amperes), the reset circuitry removes plate voltage and filament voltage from the X-ray tube and requires the operator to return to position 4.

Line Voltage Stabilizer. - The line voltage stabilizer has the following important characteristics:

Line voltage regulation:	0.2% for line voltage variation from 95 to 130 Vac
Line frequency variation:	0.4% voltage regulation for frequency shift of 57 to 63 Hz
Load regulation:	0.1% for 0 to 100% rated load
Temperature coefficient:	0.1% per °C

Component Assembly

The components described above are assembled in a 19-inch relay rack as shown in figure 13. The X-ray tube, blower, and collimator are mounted at the test chamber shown in figure 14. The proportional counter, gas supply, and preamplifier are also mounted to the test chamber. Power and signal cables are supplied from the relay rack to the test chamber. The system wiring diagram and power interconnect diagram are shown in Figure 15.

SYSTEM ANALYSIS

The basic parameters of the density measurement system are related by

$$\rho = \frac{1}{\mu x} \ln \frac{I_o}{I_d - I_b} \qquad (6)$$

where I_d is the output pulse rate; μ, ρ, and x are the mass absorption coefficient, density, and path length of the gas being measured; I_o is the equivalent pulse rate at zero density; and

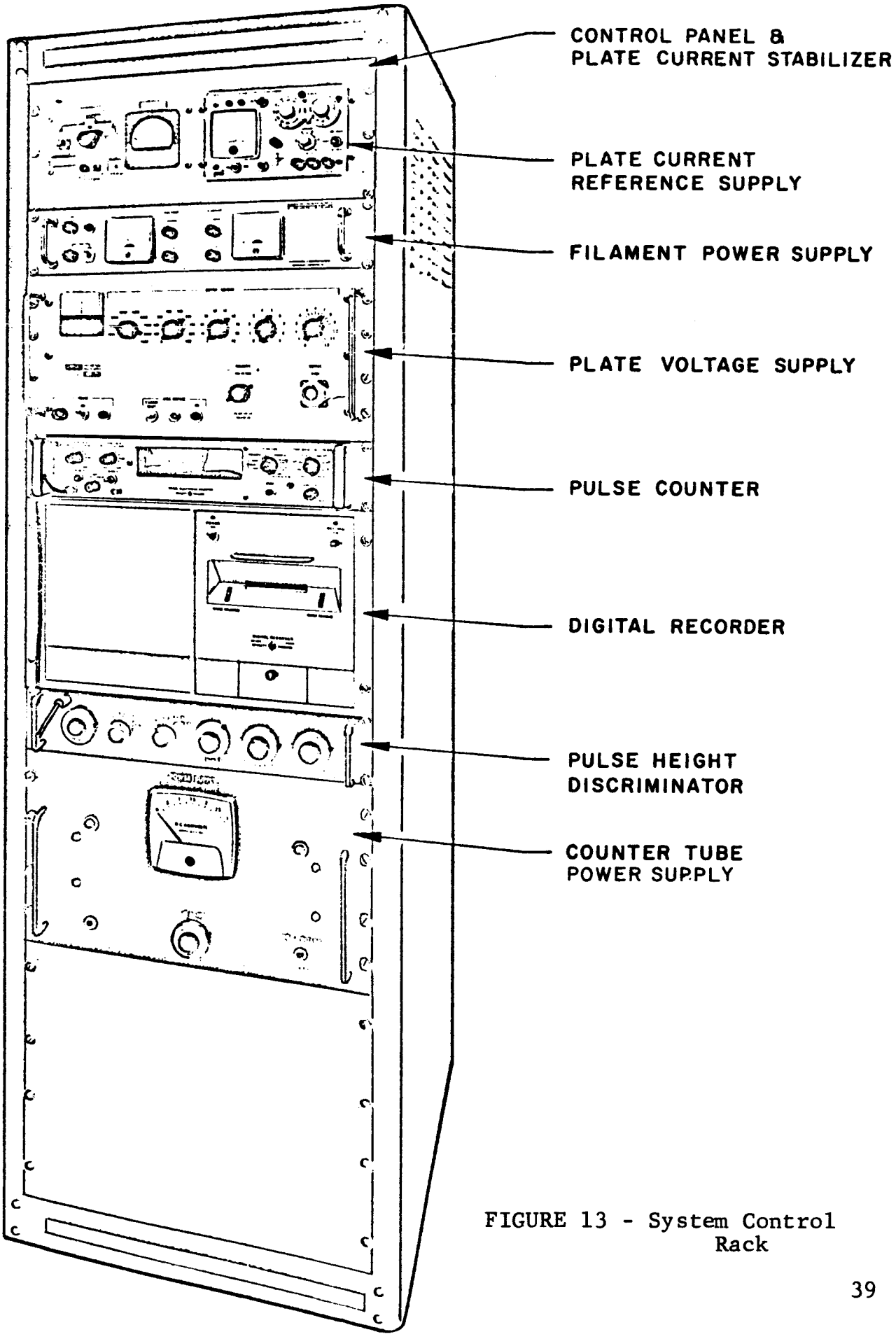

FIGURE 13 - System Control Rack

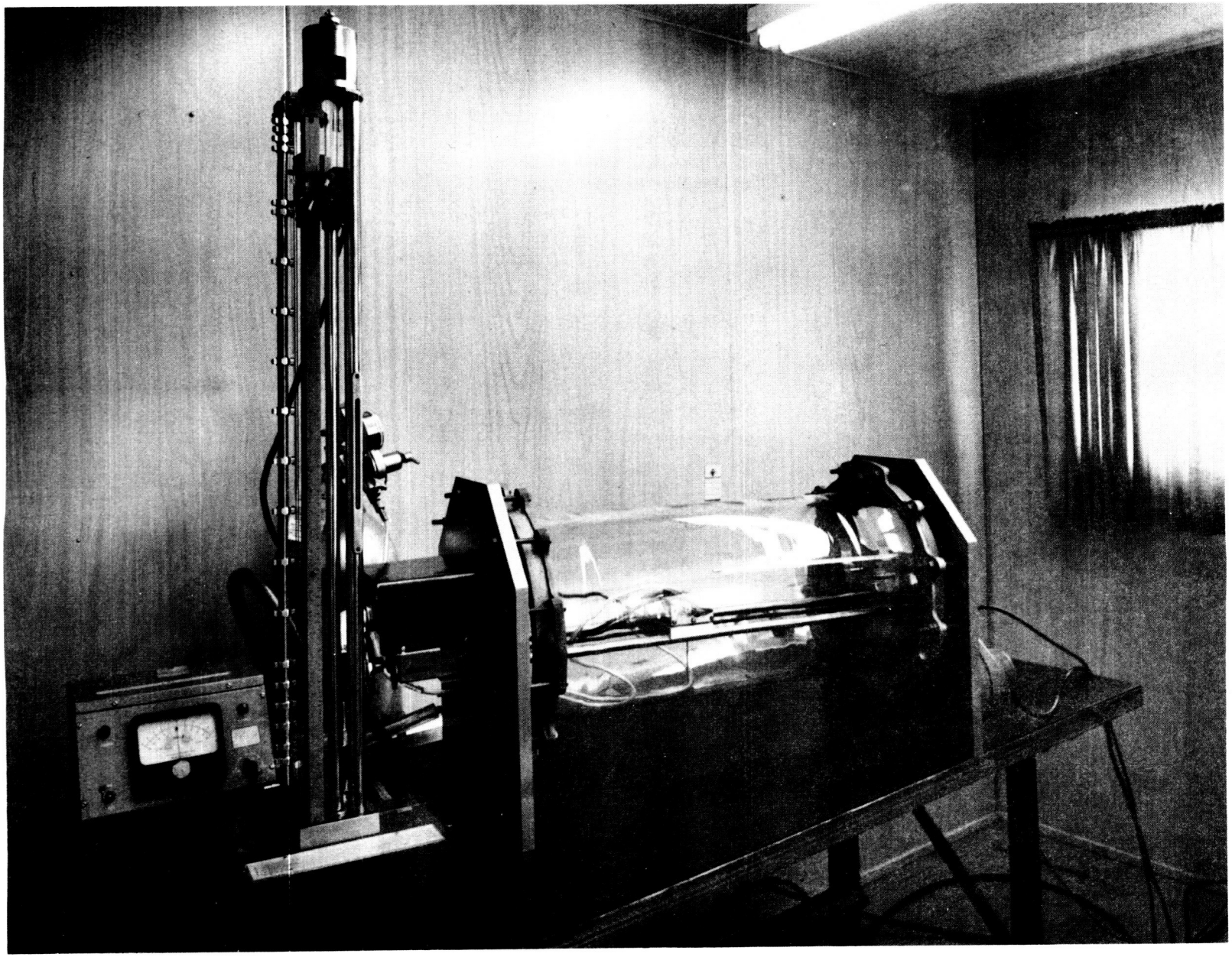

FIGURE 14 - Photograph of Calibration Chamber

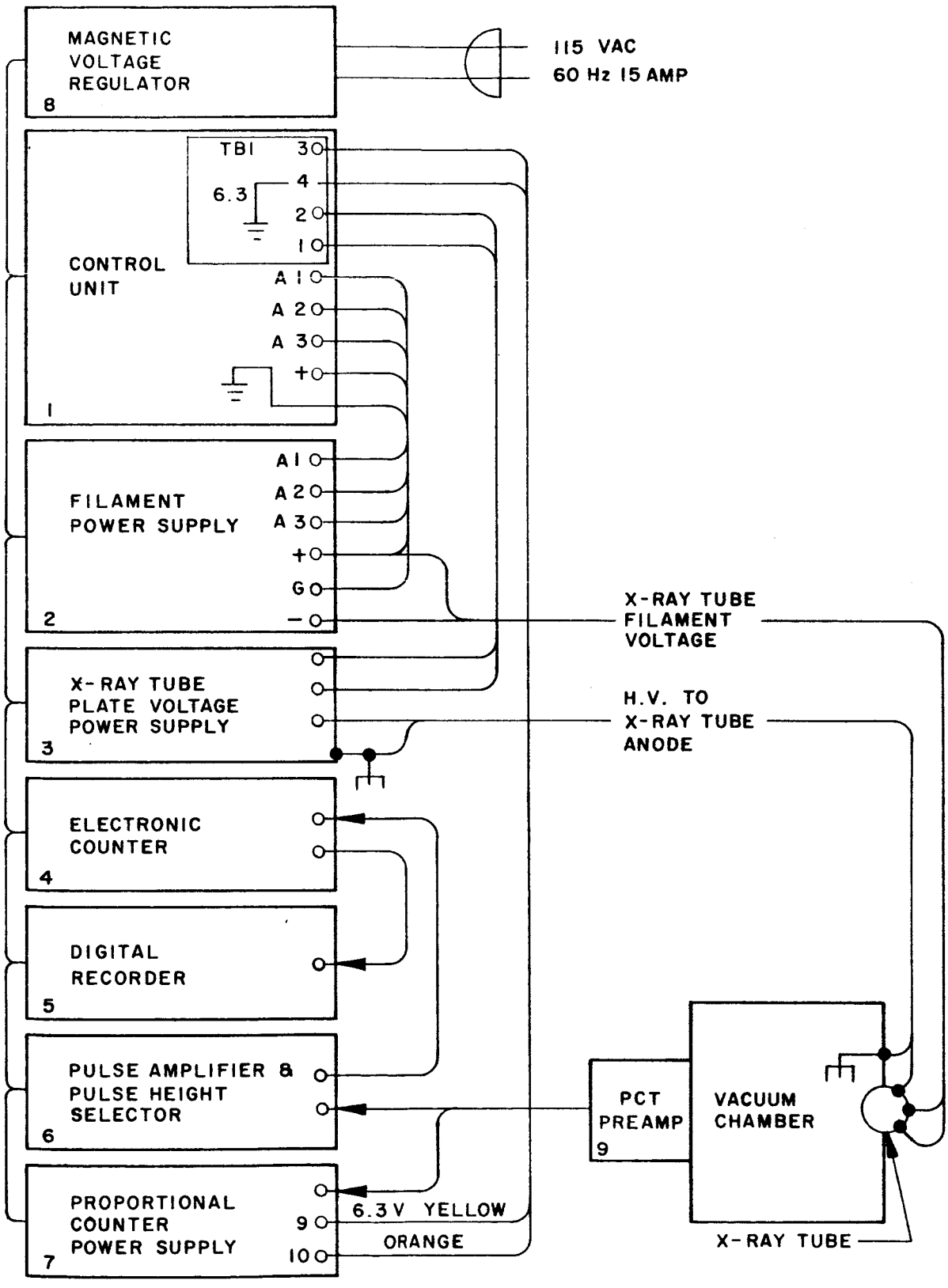

FIGURE 15a - System Wiring Diagram

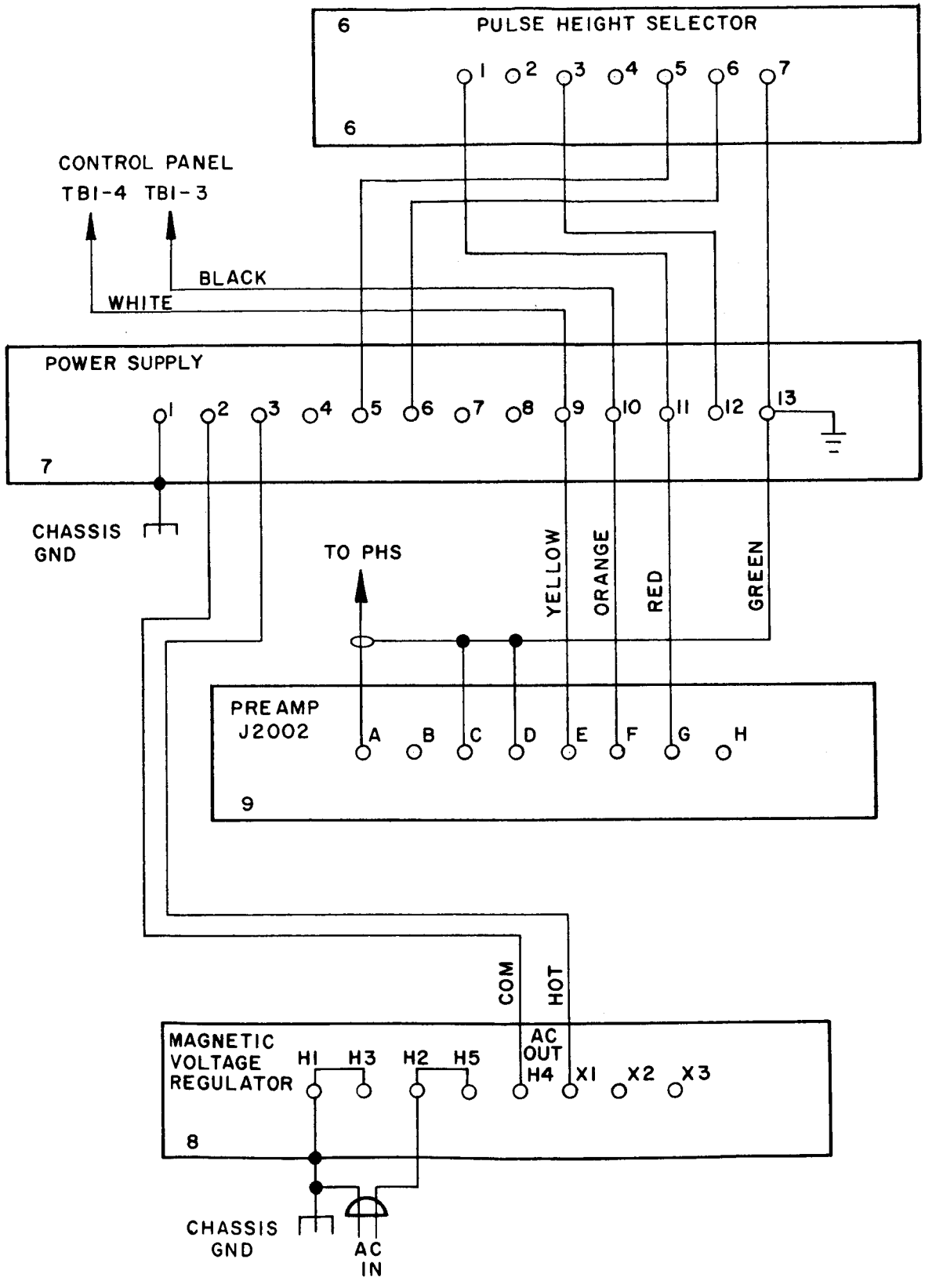

FIGURE 15b - Power Interconnect Wiring Diagram

I_b is the background pulse rate. The system is calibrated such that the relation between I_d and ρ are precisely known for the selected values of I_o, μ, and x. The accuracy of the system is dependent upon how well the calibration data repeats. There are numerous factors which affect the system calibration. These factors will be examined individually to determine the overall system accuracy.

Factors Affecting μ

Errors in the mass absorption coefficient, μ, cause errors in the density measurement as

$$\frac{\Delta\rho}{\rho} = -\frac{\Delta\mu}{\mu} \tag{7}$$

The factors affecting μ are the X-ray energy and gas composition.

X-ray Energy. - The mass absorption coefficient of air is related to the X-ray energy by the expression

$$\mu = 3800\ E^{-2.88} \tag{8}$$

obtained by examination of figure 3. Error in energy thus affects μ as

$$\frac{\Delta\mu}{\mu} = -2.88\ \frac{\Delta E}{E} \tag{9}$$

Since the X-ray energy is directly proportional to the X-ray tube plate voltage, V_p

$$\frac{\Delta\mu}{\mu} = -2.88\ \frac{\Delta V_p}{V_p} \tag{10}$$

Combining equations (7) and (10) gives

$$\frac{\Delta\rho}{\rho} = 2.88 \frac{\Delta V_p}{V_p} \tag{11}$$

Gas Composition. - The composition of air being measured is assumed to not vary.

Factors Affecting I_o

Errors in the initial X-ray flux, I_o, cause errors in the density measurement as

$$\frac{\Delta\rho}{\rho} = \frac{1}{\mu\rho x} \frac{\Delta I_o}{I_o} \tag{12}$$

The major factors affecting the initial X-ray flux detected are the X-ray tube plate voltage, the X-ray tube plate current, and the detector response.

X-ray Tube Plate Voltage. - The X-ray tube plate voltage affects the output flux by two mechanisms. The first is the X-ray generation and the second is X-ray absorption in the tube window.

From equation (4) the X-ray output intensity, I_o, is seen to be directly proportional to voltage V_p^2. Thus, variations in voltage affect density as

$$\frac{\Delta\rho}{\rho} = \frac{2}{\mu\rho x} \frac{\Delta V_p}{V_p} \tag{13}$$

The absorption of the X-ray flux in the thin beryllium window is a function of the X-ray energy or tube voltage. This relation is given as

$$I_o = I_i \, e^{-\mu_w \rho_w x_w} \tag{14}$$

and

$$\mu_w = 620\ E^{-2.88} \text{ (from data Ref. 2)} \tag{15}$$

where I_i is the initial flux, μ_w, ρ_w, and x_w are the mass absorption coefficient, density, and thickness of the beryllium window. From equations (12) (14), and (15) the voltage effect on density is found to be

$$\frac{\Delta\rho}{\rho} = -\frac{\mu_w \rho_w x_w}{\mu\rho x}\ 2.88\ \frac{\Delta V_p}{V_p} \tag{16}$$

X-ray Tube Plate Current. - Referring to equation (4), the X-ray tube output flux is seen to be directly proportional to plate current, i_p. From equations (4) and (7) the plate current affects the density measurement by

$$\frac{\Delta\rho}{\rho} = \frac{1}{\mu\rho x}\ \frac{\Delta i_p}{i_p} \tag{17}$$

The plate current is stabilized by the stabilization loop illustrated in figure 16. Errors in plate current are caused by variations in reference voltage, V_r, input resistor value, R_i, feedback resistor value, R_f, integrator capacitor leakage resistance, R_{cl}, and integrator amplifier offset voltage, V_o. These error sources are related to plate current by the following equations. The reference voltage, input resistors, and feedback resistors affect the plate current directly.

$$\frac{\Delta i_p}{i_p} = \frac{\Delta V_r}{V_r} - \frac{\Delta R_i}{R_i} - \frac{\Delta R_f}{R_f} \tag{18}$$

The integrator capacitor leakage resistance causes an error dependent upon the reference voltage, V_r, integrator output

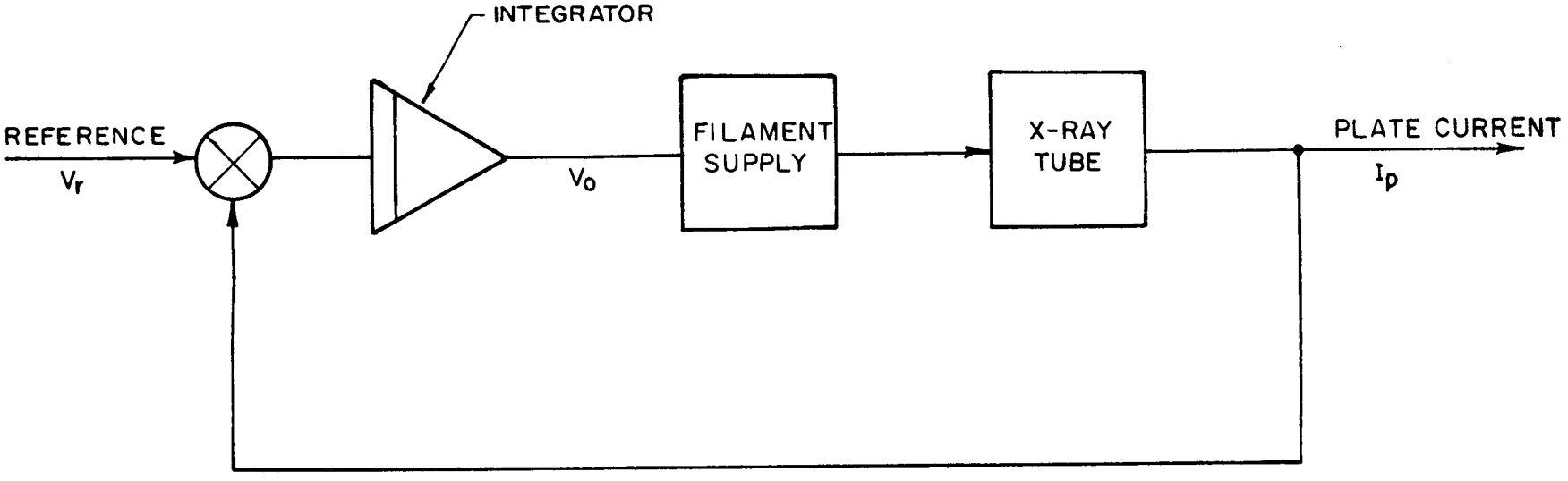

FIGURE 16 - X-ray Tube Plate Current Stabilization Loop

voltage, V_f, and input resistor value, R_i, and leakage resistance value, R_{cl}. The error due to variations in the value of leakage resistance is

$$\frac{\Delta i_p}{i_p} = \frac{R_i}{R_{cl}} \frac{V_f}{V_r} \tag{19}$$

The integration amplifier offset voltage, V_o, causes an error dependent upon the reference voltage, V_r.

$$\frac{\Delta i_p}{i_p} = \frac{V_o}{V_r} \tag{20}$$

The combined effect on density is

$$\frac{\Delta \rho}{\rho} = \frac{1}{\mu \rho x} \left[\frac{\Delta V_r}{V_r} - \frac{\Delta R_i}{R_i} - \frac{\Delta R_f}{R_f} + \frac{R_i}{R_{cl}} \frac{V_f}{V_r} + \frac{V_o}{V_r} \right] \tag{21}$$

Detection. - The sensitivity of the detector system is related to the gain and efficiency of the proportional counter, the gain of the preamplifier, and the stability of the pulse height discriminator low level setting.

The efficiency, ε, of the proportional counter is related to the counter gas density, ρ_c, as

$$\varepsilon = 1 - e^{-\mu_c \rho_c x_c} \tag{22}$$

where μ_c and x_c are the mass absorption coefficient and path length of counter gas. Variation in efficiency as a function of counter gas density is

$$\frac{\Delta \varepsilon}{\varepsilon} = \frac{\mu_c \rho_c x_c}{e^{\mu_c \rho_c x_{c-1}}} \frac{\Delta \rho_c}{\rho_c} \tag{23}$$

The counter gas density is directly proportional to pressure and equal to atmospheric pressure, P_a. Thus variations in

atmospheric pressure cause variations in efficiency as:

$$\frac{\Delta\epsilon}{\epsilon} = \frac{\mu_c \rho_c x_c}{e^{\mu_c \rho_c x_c} - 1} \frac{\Delta P_a}{P_a} \tag{24}$$

The variation of detected count rate with gain and level setting depends strongly on the detected X-ray spectrum. Figure 17 shows typical spectra in the vicinity of the base level setting normalized to the same total count rate, I_d. The discriminator base level is set at V_b. At this point the differential count rate is $\Delta I_d/\Delta V_b$. The effect of gain variations on detected count rate is thus

$$\frac{\Delta I_d}{I_d} = \left(\frac{\Delta I_d}{\Delta V_b}\right) \frac{V_b}{I_d} \frac{\Delta K}{K} \tag{25}$$

The value $\left(\frac{\Delta I_d}{\Delta V_b}\right) \frac{V_b}{I_d}$ is about the same for all spectra. Let this value be S. Then

$$\frac{\Delta I_o}{I_o} = S \frac{\Delta K}{K} \tag{26}$$

Gain variations are caused by counter tube high voltage variation, ΔV_c, preamplifier gain variation, ΔK_a, and discriminator gain variation, ΔK_b. The counter tube gain variation is related to the voltage variation as

$$\frac{\Delta K_c}{K_c} = 13.2 \frac{\Delta V_c}{V_c} \tag{27}$$

The preamplifier and discriminator gains, variations, ΔK_a and ΔK_b, have the same effect as counter tube gain variations.

Variations in the low level discriminator setting cause

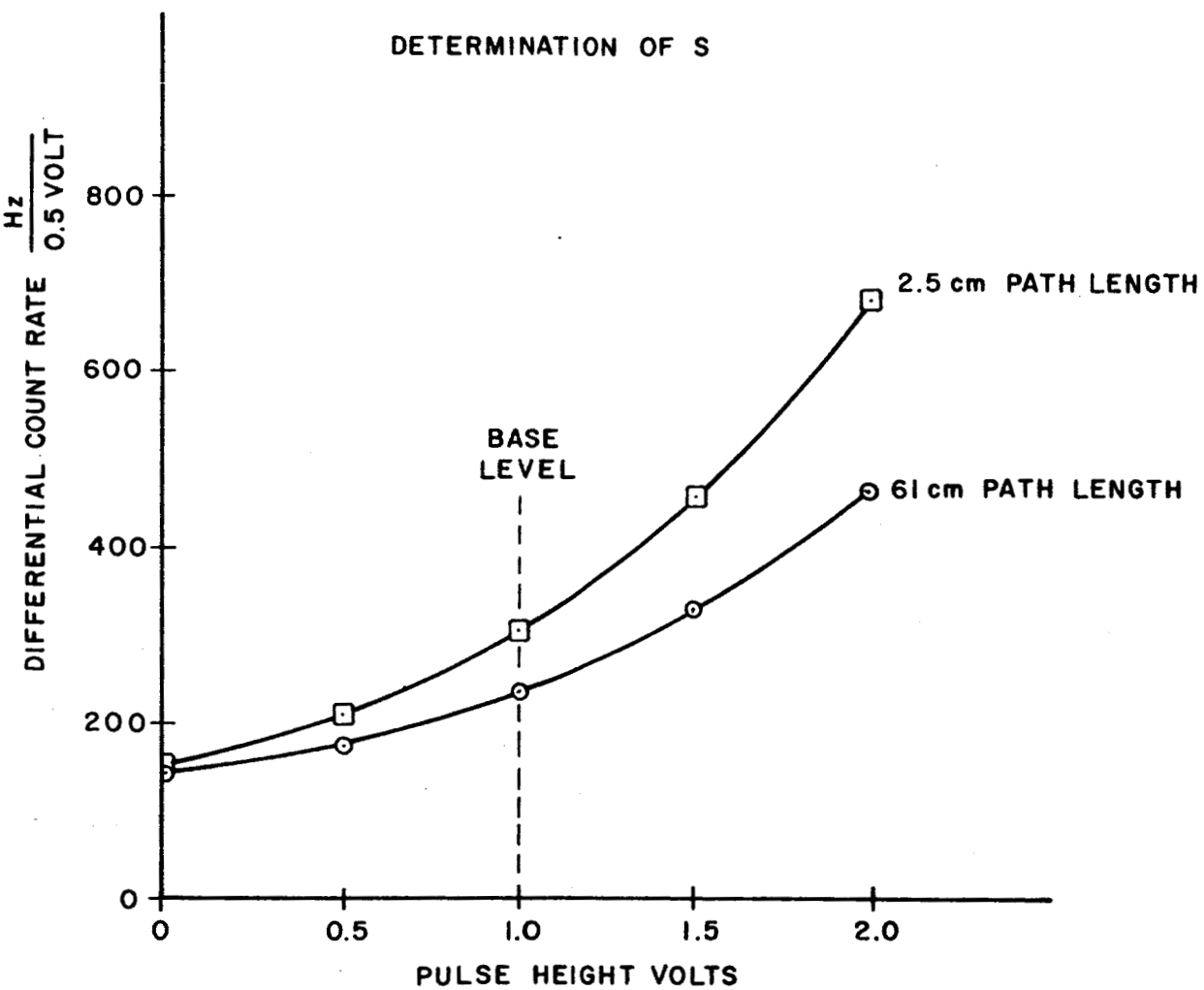

FIGURE 17 - Differential X-ray Spectrum
in Region of Base Level

variations in count rate as

$$\frac{\Delta I_o}{I_o} = -S \frac{\Delta V_b}{V_b} \tag{28}$$

The total effect of these gains, efficiency, and level variation on the density measurement are

$$\frac{\Delta \rho}{\rho} = \frac{1}{\mu \rho x} \left[\frac{u_c \rho_c x_c}{\left(e^{\mu_c \rho_c x_c} - 1 \right)} \frac{\Delta P_a}{P_a} + S \frac{\Delta K_a}{K_a} + S \frac{\Delta K_b}{K_b} + S\ 13.2 \frac{\Delta V_c}{V_c} - S \frac{\Delta V_b}{V_b} \right] \tag{29}$$

Variations in gain with count rate and pulse coincidence loss with count rate do not cause system error since they are part of the calibration.

The random nature of X-ray generation causes the number of pulses counted during a given period to fluctuate in a random fashion about an average value. Counting for a one-second interval can yield only an estimate of the true average counting rate. If the number of counts, n, is large, the standard deviation is about equal to $\pm \sqrt{n}$. For a one-second counting period, the value of n is equal to the counting rate I_d. The fractional error in count rate is then

$$\frac{\Delta I_d}{I_d} = \pm \frac{\sqrt{I_d}}{I_d} \tag{30}$$

The effect on density is then

$$\frac{\Delta \rho}{\rho} = \pm \frac{1}{\mu \rho x} \frac{\sqrt{I_d}}{I_d} \tag{31}$$

Calibration. - System calibration is performed in a vacuum chamber with carefully controlled and measured density. For every path length, with the exception of 2.5 cm, the plate

voltage and current are determined to give a calibration curve which has a pulse rate of 200 Hz at 1 atmosphere and 80,000 Hz at 0.01 atmosphere. For the 2.5 cm path length, the plate current and voltage are determined to give a 100 Hz pulse rate at 1.0 atmosphere and 40,000 Hz pulse rate at 0.01 atmosphere.

Thirty-second counting periods are used to improve the counting statistics for the calibration. The calibration uncertainty due to counting statistics is thus

$$\frac{\Delta I_d}{I_d} = \pm \frac{\sqrt{30\ I_d}}{30\ I_d} \tag{32}$$

Relating to density gives

$$\frac{\Delta \rho}{\rho} = \pm \frac{1}{\mu \rho x} \frac{\sqrt{30\ I_d}}{30\ I_d} \tag{33}$$

The calibration data is plotted on log-log paper to sufficient size such that reading error is less than ±1% of density.

$$\frac{\Delta \rho}{\rho} = \pm\ 0.01 \tag{34}$$

The density of the air in the calibration chamber is computed from pressure and temperature measurements. The pressure measurement is made to an accuracy of better than ±0.35% of reading and the temperature measurement to better than ±0.17% of reading. The density is computed from the equation

$$\rho = \frac{P}{RT} \tag{35}$$

where ρ is the density, P is the measured pressure, T is the measured temperature, and R is the gas constant. Errors in pressure and temperature measurement affect density as

$$\frac{\Delta\rho}{\rho} = \frac{\Delta P}{P} - \frac{\Delta T}{T} \tag{36}$$

The water content of the air being measured will cause a slight error in the computation of density due to the difference in gas constants.

The measured pressure P is the sum of the partial pressures of water vapor P_w and air P_a.

$$P = P_w + P_a \tag{37}$$

The density of the gas ρ is the sum of the density of the water vapor ρ_w and air ρ_a

$$\rho = \rho_w + \rho_a \tag{38}$$

The computation of density of each component is

$$\rho_w = \frac{P_w}{R_w T} \tag{39}$$

$$\rho_a = \frac{P_a}{R_a T} \tag{40}$$

The density of the mixture is then

$$\rho = \frac{P_w}{R_w T} + \frac{P_a}{R_a T} \tag{41}$$

The density used in the calibration, ρ_c, assumed no moisture content

$$\rho_c = \frac{P}{R_a T} \tag{42}$$

The relative error in density is thus

$$\frac{\Delta\rho}{\rho} = \frac{\rho_c - \rho}{\rho_c} = \frac{P_w}{T}\left(1 - \frac{R_a}{R_w}\right) \tag{43}$$

For a typical condition of 40% relative humidity, a temperature of 25°C, and a pressure of one atmosphere, the ratio $\frac{P_w}{P_a} = 0.0125$. The ratio of gas constant $\frac{R_a}{R_w} = 0.62$. The error in density is thus

$$\frac{\Delta\rho}{\rho} = 0.0125\ (1 - .62) = 0.0048 \tag{44}$$

An additional error is introduced due to the different mass absorption coefficient of water vapor than air. The fractional error in density due to this effect is given by

$$\frac{\Delta\rho}{\rho} = \frac{P_w}{P_a}\left(\frac{\mu_w}{\mu_a} - 1\right) \tag{45}$$

For the case with 40% relative humidity, the ratio of densities is $\frac{\rho_w}{\rho_a} = 0.0125$ and the ratio of mass absorption coefficients is $\frac{\mu_w}{\mu_a} = 1.04$ the error is

$$\frac{\Delta\rho}{\rho} = 0.0125\ (1.04 - 1) = +0.0005. \tag{46}$$

Inaccuracies in setting up the path length during calibration causes density errors given by

$$\frac{\Delta\rho}{\rho} = -\frac{\Delta x}{x} \tag{47}$$

Background. - The background pulse rate I_b is less than 2 pulses per second. The fractional error in density caused, assuming no background correction, is given by

$$\frac{\Delta\rho}{\rho} = \frac{1}{\mu\rho x}\frac{I_b}{I_d} \tag{48}$$

Error Summary. - The individual errors are listed in table I.

TABLE I. - ERROR SUMMARY

61 cm Path Length

Error Source	Equa. No.	Parameter Uncertainty	Multiplying Factor	0.01 Atmosphere: Parameter Uncertainty	0.01 Atmosphere: Multiplying Factor	0.01 Atmosphere: % Error in Density	0.1 Atmosphere: Parameter Uncertainty	0.1 Atmosphere: Multiplying Factor	0.1 Atmosphere: % Error in Density	1.0 Atmosphere: Parameter Uncertainty	1.0 Atmosphere: Multiplying Factor	1.0 Atmosphere: % Error in Density
X-ray tube plate voltage effects on σ	(11)	$\Delta V/V$	+2.88	±0.05%	+2.88			+2.88			+2.88	
X-ray tube plate voltage effects on flux generation	(13)	$\Delta V/V$	$+\frac{2}{\mu\rho x}$	±0.05%	+11.76	±0.85		+2.54	±0.30		+0.778	±0.17
X-ray tube plate voltage effects on window absorption	(16)	$\Delta V/V$	$+\frac{\mu_w\rho_w x_w}{\mu\rho x}2.88$	±0.025%	+4.71			-1.18			+0.151	
Reference voltage effects on X-ray tube plate current	(21)	$\frac{\Delta V_r}{V_r}$	$+\frac{1}{\mu\rho x}$	±0.2%	+5.88	±1.18		+1.27	±0.254		+0.189	±0.0378
Input resistor effects on X-ray tube plate current	(21)	$\frac{\Delta R_i}{R_i}$	$-\frac{1}{\mu\rho x}$	±0.125%	-5.88	±0.736		-1.27	±0.159		-0.189	±0.0236
Feedback resistor effects on X-ray tube plate current	(21)	$\frac{\Delta R_f}{R_f}$	$-\frac{1}{\mu\rho x}$	±0.125%	-5.88	±0.736		-1.28	±0.159		-0.189	±0.189
Integration capacitor leakage effects on X-ray tube plate current	(21)	$\frac{1}{R_{cl}}$	$+\frac{1}{\mu\rho x}R_i\frac{V_f}{V_r}(100\%)\,10^{-9}\,\text{ohm}^{-1}$	+16x10$^7\Omega$%		±0.16		+4.3x10$^7\Omega$%	±0.043		+0.64x10$^7\Omega$%	±0.006
Integration amplifier offset voltage effects on X-ray tube plate current	(21)	V_o	$+\frac{1}{\mu\rho x}\frac{1}{V_r}(100\%)$	±50x10^{-6}v	+1.06x10^{6}v^{-1}%	±0.53		+.231x10^{6}v^{-1}%	±0.115		+.034x10^{6}v^{-1}%	±0.017
Atmospheric pressure effects on counter tube efficiency	(29)	$\frac{\Delta P_a}{P_a}$	$+\frac{\mu_c\rho_c x_c}{e^{\mu_c\rho_c x_c}-1}\frac{1}{\mu\rho x}$	±1.0%	+1.58	±1.58		+.341	±0.341		+.051	±0.051
Counter tube voltage effects on counter tube gain	(29)	$\frac{\Delta V_c}{V_c}$	$+\frac{S\,13.2}{\mu\rho x}$	±0.035%	+.385	±0.0135		+.083	±0.0029		+.00123	±4.3x10^{-5}
Preamplifier gain effects on detection	(29)	$\frac{\Delta K_a}{K_a}$	$+\frac{S}{\mu\rho x}$	±0.5%	+.0294	±0.015		+.00635	±0.0032		+.00095	±0.00048
Discriminator gain effects on Detection	(29)	$\frac{\Delta K_b}{K_b}$	$+\frac{S}{\mu\rho x}$	±0.5%	+.0294	±0.015		+.00635	±0.0032		+.00095	±0.00048
Discriminator level setting effects on detection	(29)	$\frac{\Delta V_b}{V_b}$	$-\frac{S}{\mu\rho x}$	±30%	-.0294	±0.87		-.00635	±0.189		-.00095	±0.028
Random pulse rate effects on detection	(31)	$\frac{\sqrt{I_d}}{I_d}$	$\pm\frac{1}{\mu\rho x}$	±0.5%	±5.88	±2.06	±0.61	±1.27	±0.445	±7.05	±0.189	±1.33
Random pulse rate effects on calibration	(33)	$\frac{\sqrt{301_d}}{301_d}$	$\pm\frac{1}{\mu\rho x}$	±0.091%	±5.88	±0.37	±0.111	±1.27	±0.08	±1.28	±0.189	±0.24
Calibration chart reading error effect on density		±0.01	+1.0	±1.0%	+1.0	±1.0		+1.0	±1.0		+1.0	±1.0
Pressure measurement effect on calibration	(36)	$\frac{\Delta P}{P}$	+1.0	±0.35%	+1.0	±0.35		+1.0	±0.35		+1.0	±0.35
Temperature measurement effect on calibration	(36)	$\frac{\Delta T}{T}$	-1.0	±0.17%	-1.0	±0.17		-1.00	±0.17		-1.0	±0.17
Humidity effects on calibration pressure	(43)	$\frac{P_w}{P}$	$+\left(1-\frac{R_a}{R_w}\right)$	+1.25%	+0.38	+0.475		+0.38	+0.475		+0.38	+0.475
Humidity effects on calibration absorption	(45)	$\frac{P_w}{P}$	$+\left(\frac{\mu_w}{\mu_a}-1\right)$	+1.25%	+0.04	+0.05		+0.04	+0.05		+0.04	+0.05
Path length effects on calibration	(47)	$\frac{\Delta x}{x}$	-1.0	±0.02%	-1.0	±0.02		-1.0	±0.02		-1.0	±0.02
Background effects on density	(48)	$\frac{I_b}{I_d}$	$+\frac{1}{\mu\rho x}$	±2.5x10^{-3}%	+5.88	±0.0015	±7.4x10^{-3}%	+1.27	±0.0094	±1.0%	+0.189	±0.189
			TOTAL	2σ Error		±3.5%			±2.74			±3.01

CONSTANTS

V_p 4750 V

$\frac{1}{\mu\rho x}$ 5.88 1.27 0.189

$\mu_w\rho_w x_w$ 12x1.82x0.005x2.54 0.277

I_p 0.398 mA

V_r 0.0398 volts

V_o = filament voltage 3 volts

$\mu_c\rho_c x_c$ = 500x.00178 x 2.5 = 2.23

S = 0.005

$\frac{\partial K_a/\partial V_c}{K_a/V_c}$ = 13.2

I_d = 80.000 Hz 27,000 Hz 200 Hz

I_b = 2 Hz

R_i = 6200

TABLE I. - ERROR SUMMARY

2.5 cm Path Length

Error Source	Equa. No.	Parameter Uncertainty	Multiplying Factor	0.01 Atmosphere: Parameter Uncertainty	0.01 Atmosphere: Multiplying Factor	0.01 Atmosphere: % Error in Density	0.1 Atmosphere: Parameter Uncertainty	0.1 Atmosphere: Multiplying Factor	0.1 Atmosphere: % Error in Density	1.0 Atmosphere: Parameter Uncertainty	1.0 Atmosphere: Multiplying Factor	1.0 Atmosphere: % Error in Density
X-ray tube plate voltage effects on μ	(11)	$\Delta V/V$	+2.88	±0.05%	+2.88			+2.88			+2.88	
X-ray tube plate voltage effects on flux generation	(13)	$\Delta V/V$	$+\frac{2}{\mu\rho x}$	±0.05%	+32	±7.0		3.2	±1.07		+0.33	±0.215
X-ray tube plate voltage effects on window absorption	(16)	$\Delta V/V$	$-\frac{\mu_w \rho_w x_w}{\mu\rho x}$ 2.88	±0.025%	+213			+30.7			+2.2	
Reference voltage effects on X-ray tube plate current	(21)	$\frac{\Delta V_r}{V_r}$	$+\frac{1}{\mu\rho x}$	±0.0065%	+16	±0.104		+1.6	±0.01		+0.165	±0.0011
Input resistor effects on X-ray tube plate current	(21)	$\frac{\Delta R_1}{R_1}$	$-\frac{1}{\mu\rho x}$	±0.125%	-16	±2.0		-1.6	±0.20		-0.165	±0.021
Feedback resistor effects on X-ray tube plate current	(21)	$\frac{\Delta R_f}{R_f}$	$-\frac{1}{\mu\rho x}$	±0.125%	-16	±2.0		-1.6	±0.20		-0.165	±0.021
Integration capacitor leakage effects on X-ray tube plate current	(21)	$\frac{1}{R_{cl}}$	$+\frac{1}{\mu\rho x} R_1 \frac{V_f}{V_r} (100\%)$	10^{-9} ohm^{-1}	+5.4x10^7	±0.054		+5.4x10^6	±0.005		+5.6x10^5	±0.0006
Integration amplifier offset voltage effects on X-ray tube plate current	(21)	V_o	$+\frac{1}{\mu\rho x}\frac{1}{V_r}(100\%)$	±50x10^{-6}V	+2040V^{-1}%	+0.102		+203V^{-1}%	±0.0103		+21V^{-1}%	±0.001
Atmospheric pressure effects on counter tube efficiency	(29)	$\frac{\Delta P_a}{P_a}$	$+\frac{\mu_c \rho_c x_c}{\mu_c \rho_c x_c - 1}\frac{1}{\mu\rho x}$	±1.0%	+0.534	±0.534		±0.053	±0.053		+0.0055	±0.0055
Counter tube effects on counter tube gain	(29)	$\frac{\Delta V_c}{V_c}$	$+\frac{S\ 13.2}{\mu\rho x}$	±0.035	+1.06	±0.037		+0.105	±0.0037		+0.0109	±0.00038
Preamplifier gain effects on detection	(29)	$\frac{\Delta K_a}{K_a}$	$+\frac{S}{\mu\rho x}$	±0.5%	+0.08	±0.04		+0.0076	±0.004		+0.00082	±0.00041
Discriminator gain effects on detection	(29)	$\frac{\Delta K_b}{K_b}$	$+\frac{S}{\mu\rho x}$	±0.5%	+0.08	±0.04		+0.0076	±0.004		+0.00082	±0.00041
Discriminator level setting effects on detection	(29)	$\frac{\Delta V_b}{V_b}$	$-\frac{S}{\mu\rho x}$	±30%	-0.08	±2.4		-0.0076	±0.24		-0.00082	±0.025
Random pulse rate effects on detection	(31)	$\frac{\sqrt{I_d}}{I_d}$	$\pm\frac{1}{\mu\rho x}$	±0.5%	±16	±8.0	±0.65%	±1.6	±1.05	±10%	±0.165	±1.65
Random pulse rate effects on calibration	(33)	$\frac{\sqrt{30 I_d}}{30 I_d}$	$\pm\frac{1}{\mu\rho x}$	±0.091%	±16	±1.46	±0.162%	±1.6	±0.26	±1.82%	±0.165	±0.3
Calibration chart reading error effect on density		±0.01	+ 1.0	±1.0%	+1	±1.0		+1	±1.0		+1	±1.0
Pressure measurement effect on calibration	(36)	$\frac{\Delta P}{P}$	+ 1.0	±0.35%	+1	±0.35		+1	±0.35		+1	±0.35
Temperature measurement effect on calibration	(36)	$\frac{\Delta T}{T}$	-1.0	±0.17%	-1	±0.17		-1	±0.17		-1	±0.17
Humidity effects on calibration pressure	(43)	$\frac{P_w}{P}$	$+\left(1 - \frac{R_a}{R_w}\right)$	+1.25%	+0.38	±0.475		+0.38	±0.475		+0.38	±0.475
Humidity effects on calibration absorption	(45)	$\frac{P_w}{P}$	$+\left(\frac{\mu_w}{\mu_a} - 1\right)$	+1.25%	+0.04	±0.05		+0.04	±0.05		+0.04	±0.05
Path length effects on calibration	(47)	$\frac{\Delta x}{x}$	-1.0	±0.5%	-1	±0.5		-1	±0.5		-1	±0.5
Background effects on density	(48)	$\frac{I_b}{I_d}$	$+\frac{1}{\mu\rho x}$	5.0x10^{-3}%	+16	±0.08	±8.6x10^{-3}%	+1.6	±0.014	±2.0%	+0.165	±0.33
			TOTAL	2 σ Error		±11.4%			±1.96			±2.18

CONSTANTS

V_p	1480 V		
$\frac{1}{\mu\rho x}$	16	1.6	0.165
$\mu_w \rho_w x_w$	200 x 1.82 x 0.005 x 254 = 4.62		
I_p	7.644 mA		
V_r	0.7644 volts		
R_1	6200 Ω		
V_o	4.2 V		
$\mu_c \rho_c x_c$	5.0		
S	0.005		
$\frac{\Delta K_c}{K_c}/\frac{\Delta V_c}{V_c}$	13.2		
I_d	40.000 Hz	23,000 Hz	100 Hz
I_b	2 Hz		

The random errors are listed as ± values. The systematic errors have a single sign either + or -. The uncorrelated random errors are summed as the square root of the sum of the square and the correlated random errors are summed algebraically. The errors are computed at the distances of 2.5 cm and 61 cm, and at three densities, 1 atmosphere, 0.1 atmosphere, and 0.01 atmosphere. These total errors are summarized in table I. These errors are plotted as a function of density in figure 18. The one sigma error is less than ±5.0% in all cases.

SYSTEM PERFORMANCE

This section discusses the results of system testing showing calibration measurements, stability measurements, and repeatability measurements. The test methods are described and important results analyzed.

Calibration

The system calibration was done using the calibration chamber illustrated in figure 19. The density of the air in the chamber is controlled using a vacuum pump and bleed valves. Accurate measurement of pressure is obtained with the manometer and temperature with the thermometer. The separation distance of the source and detector is adjusted external to the chamber, using the lead screw and carriage. Repeatable positioning of the carriage is assured by use of a turn counter geared to the lead screw which reads out separation distance to the nearest 0.025 cm and can be interpolated to 0.005 cm. The counter gas

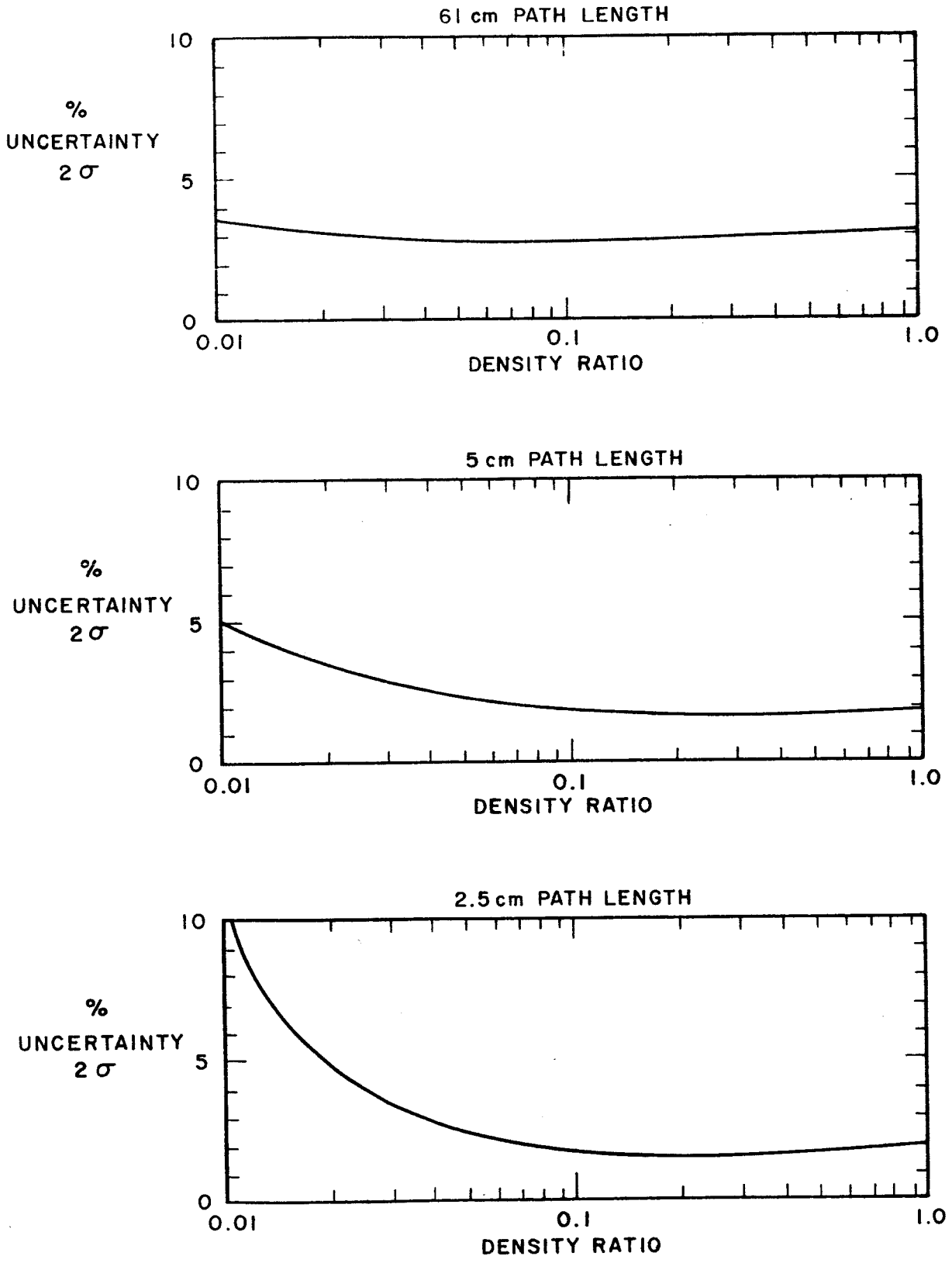

FIGURE 18 - System Error vs. Density

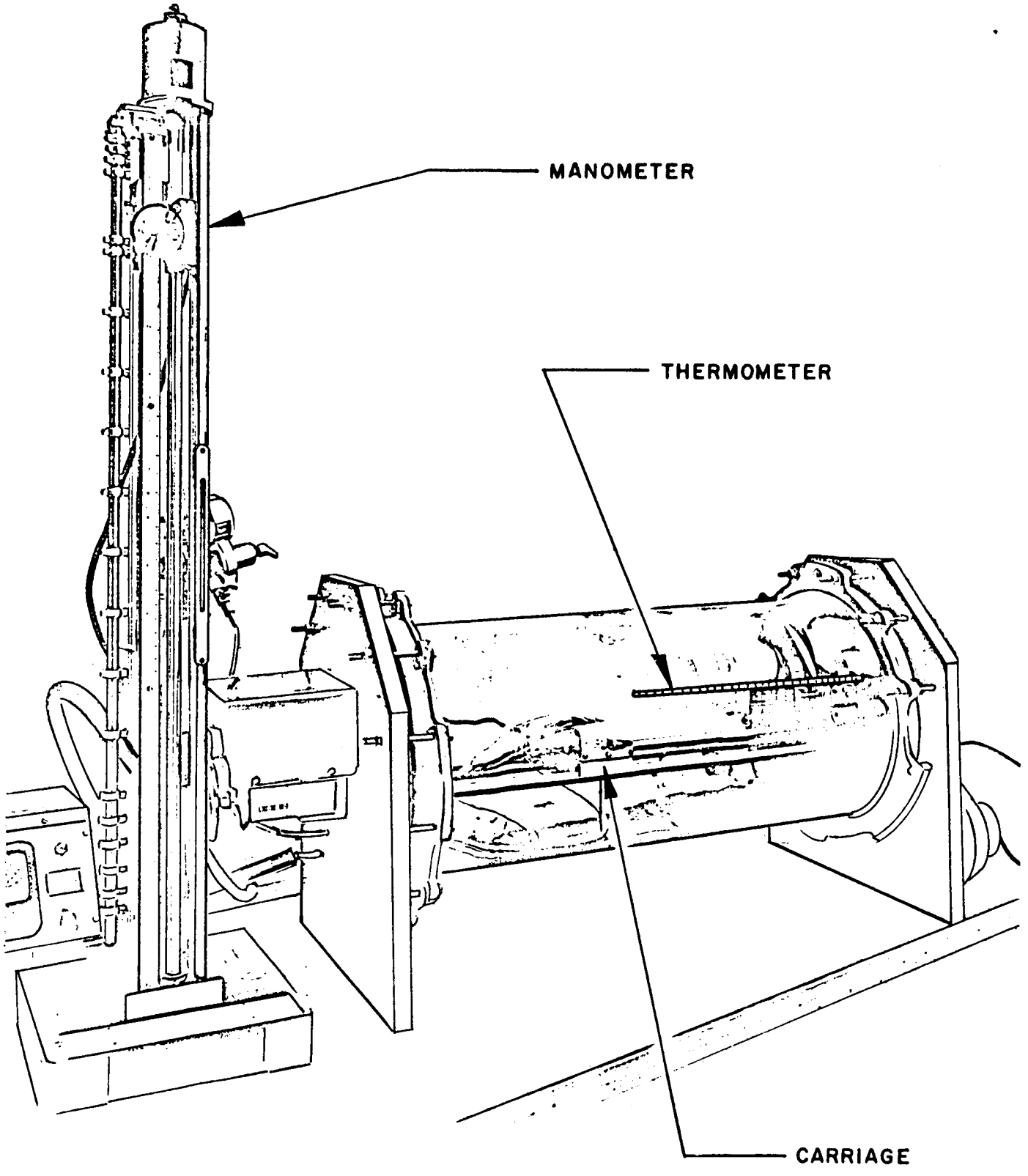

FIGURE 19 - System Calibration Setup

and high voltage reach the detector via tubing and cabling, feeding through the end plate. A blower is mounted to the opposite end plate used to cool the X-ray tube. The collimator is mounted at the X-ray tube window to an alignment plate such that adjustment of the beam alignment can be made. An access port is provided in this end plate.

The first step in system calibration is to check the equipment settings as defined in the operating instructions. The system is turned on and the collimator aligned. An X-ray photograph is taken verifying the location of the X-ray beam. The required distance is set up and, using a trial and error method, the plate current and plate voltage are determined to provide a 200 Hz count rate (less background) at a pressure of 71 cm Hg and an 80,000 Hz count rate at a pressure of 0.71 cm of Hg (100 Hz and 40,000 Hz for 2.5 cm path length). The chamber temperature is noted. With this plate current and voltage established, the calibration data of count rate versus pressure is taken, noting the chamber temperature at each point. The density is computed from the pressure and temperature measurements and count rate versus density plotted. A typical calibration curve is shown in figure 20. The data is presented as a log-log plot to give equal reading resolution in percent of reading over the entire measurement range. Table II gives the voltage and current settings for each separation distance.

The calibration curves at distances of 2.5 cm and 61 cm are shown in figure 21, plotted on semi-log paper. Notice the

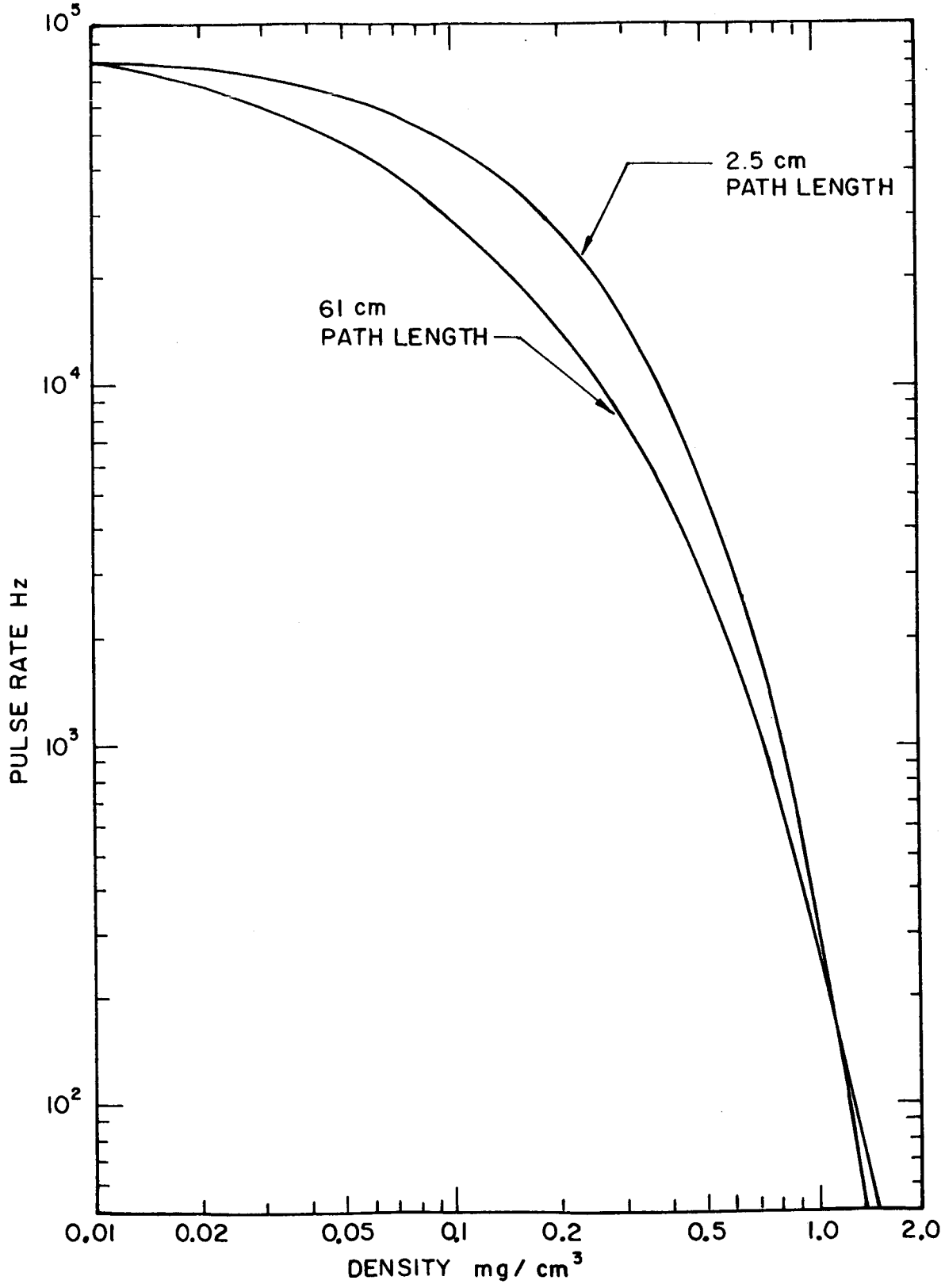

FIGURE 20 - Typical Calibration Curves

TABLE II. - CALIBRATION SETTINGS

Path Length X-ray Tube to Detector (inches)	Collimator Length (inches)	Plate Voltage (volts)	Plate Current (Ref. Volt) (mA x 10^{-1})	Time Constant Switch
1.0	0.25	1480	0.7644	Slow
1.5	0.25	1671	0.2934	Fast
2.0	0.25	1835	0.1062	Fast
2.0	0.5	1839	0.3802	Fast
3.0	0.5	2164	0.0736	Fast
4.0	0.5	2435	0.0313	Fast
5.0	0.5	2665	0.0190	Fast
5.0	1.0	2660	0.0733	Fast
6.0	1.0	2845	0.0530	Fast
7.0	1.0	3040	0.0402	Fast
8.0	1.0	3200	0.0332	Fast
9.0	1.0	3300	0.0288	Fast
10.0	1.0	3445	0.0255	Fast
10.0	2.0	3465	0.1048	Fast
11.0	2.0	3573	0.0940	Fast
12.0	2.0	3680	0.0847	Fast
13.0	2.0	3790	0.0767	Fast
14.0	2.0	3890	0.0790	Fast
15.0	2.0	3980	0.0657	Fast
16.0	2.0	4080	0.0602	Fast
17.0	2.0	4165	0.0566	Fast
18.0	2.0	4265	0.0528	Fast
19.0	2.0	4350	0.0500	Fast
20.0	2.0	4440	0.0471	Fast
21.0	2.0	4510	0.0454	Fast
22.0	2.0	4590	0.0435	Fast
23.0	2.0	4670	0.0416	Fast
24.0	2.0	4750	0.0398	Fast

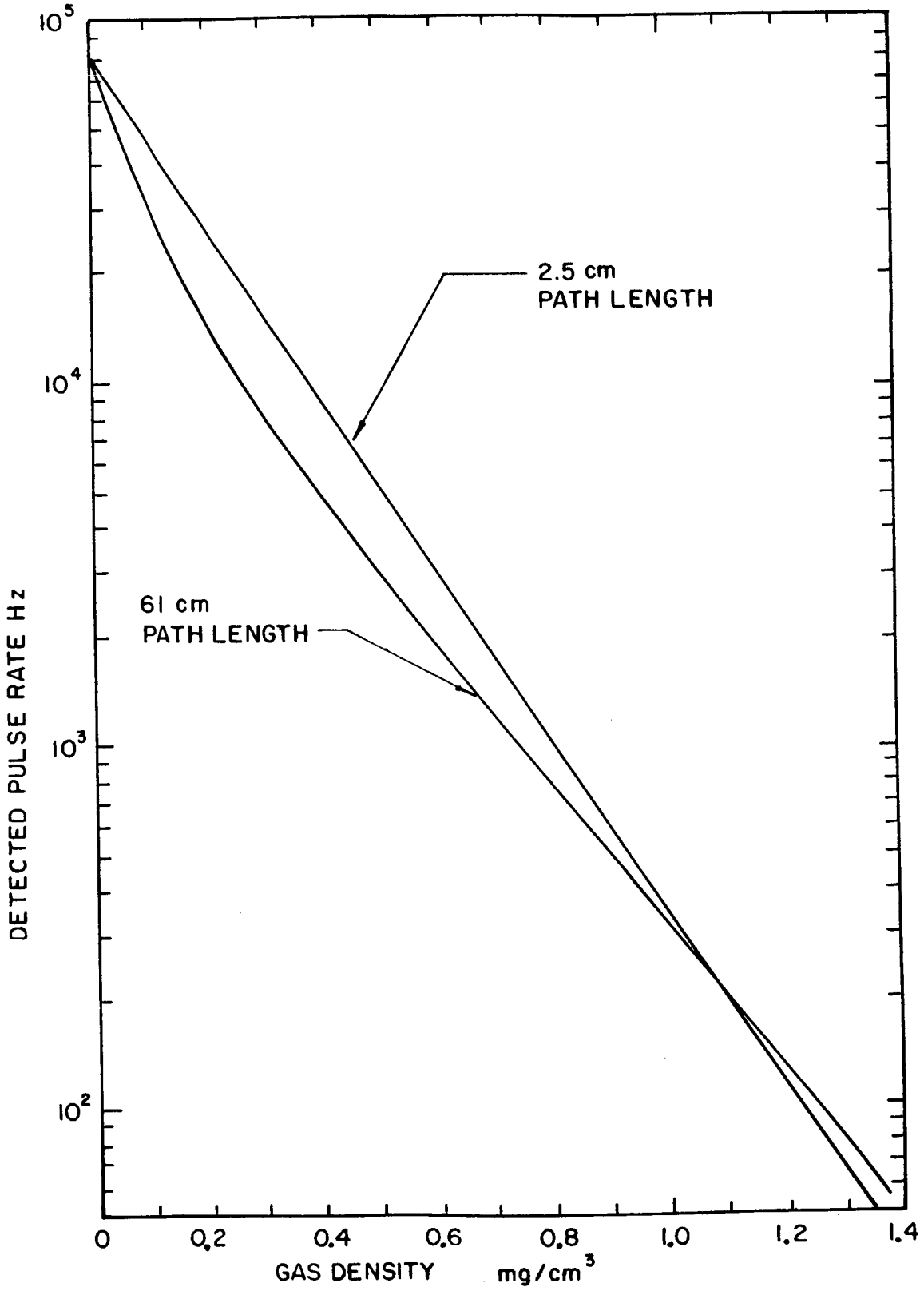

FIGURE 21 - Calibration Curves
Showing Exponential Absorption

deviation from a pure exponential absorption curve at 61 cm and the nearly perfect curve at the 2.5 cm distance. The primary reason for the large difference in shape of the two calibration curves is a peculiar dual spectrum from the X-ray tube. Figure 22 illustrates this dual spectrum at two values of density and a 61 cm distance. The upper energy spectrum is the X-ray tube continuous spectrum whose energy is variable depending upon the plate voltage. The lower energy spectrum is fixed at about 1 keV regardless of plate voltage. This spectrum is felt to be a copper L emission from copper contaminant on the face of the tungsten target. At high densities, this copper L emission is easily absorbed and the calibration curve has a slope consistent with the exponential absorption characteristic of the upper energy. At low density, the copper L emission intensity is large compared to the continuous spectrum and the calibration curve has a much steeper slope consistent with the exponential absorption characteristic of the lower energy. Thus the change in slope with density. At short path lengths, the plate voltage required is lower and the continuous spectrum falls on top of the copper L emission, giving a single line and thus a single slope to the calibration curve. Curves for intermediate distances fall between the two extremes of figure 21. System accuracy improves with a steepening of the calibration slope.

A measure of the detector response was taken to verify the coincidence loss estimate. Figure 23 shows the result of a plot of count rate versus plate current. The relationship is nearly

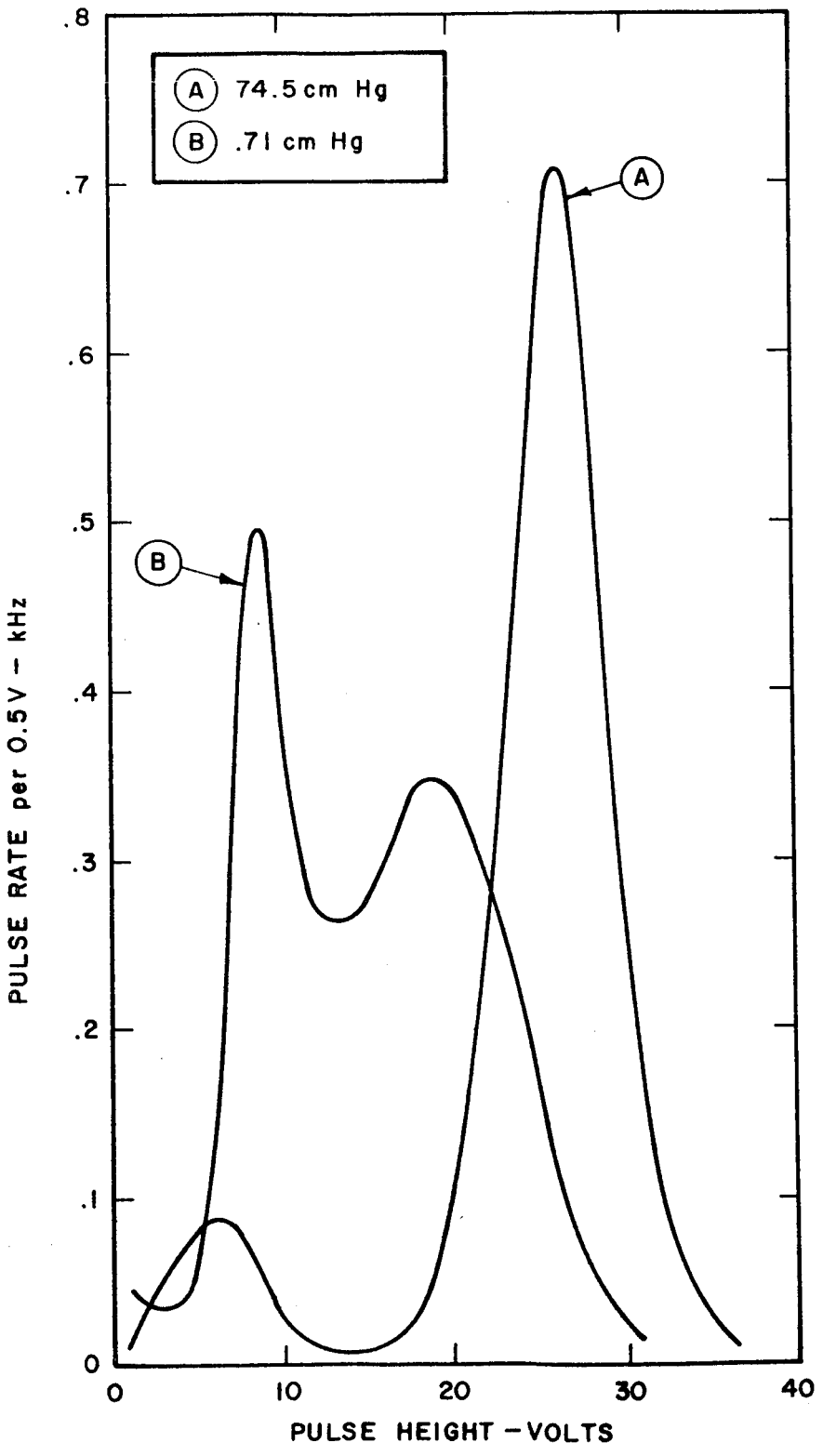

FIGURE 22 - X-ray Tube Output Spectrum Illustrating Dual Output Characteristic

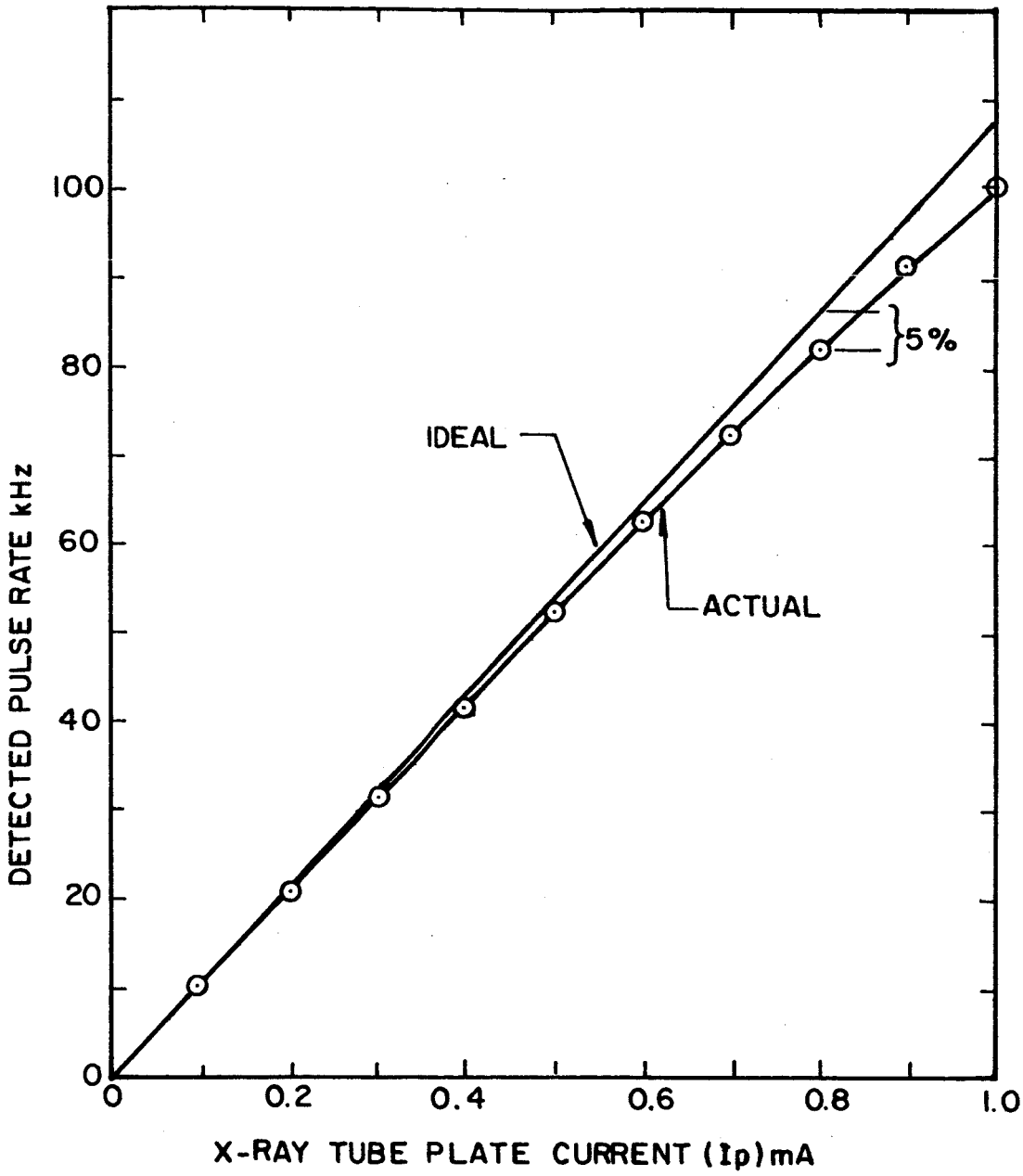

FIGURE 23 - Detector Count Rate Response

linear showing a counting loss of only 5% at a count rate of 80,000 Hz.

Stability

Stability measurements were taken to show the short and long term drifts of the system. Figure 24 shows a typical 2½ hour stability run, including system warm-up. Each data point is a 10-second average. The statistical spread is normal. The system drift is not noticeable within the ± 0.11% one sigma data spread.

Repeatability

Repeatability measurements were taken of the system by comparing repeated calibration data at several distances over a period of several weeks. Count rate measurements were made at the upper and lower ends of the calibration. The data points are averages of three 10-second counting intervals. This data is referred to density variations and plotted as a probability distribution in figure 25, showing a ±1 σ spread of ±5%.

OPERATING INSTRUCTIONS

The following section briefly describes recommended methods of system setup and operation.

System Mounting

The X-ray tube and proportional counter are mounted on opposite sides of the gas to be measured. The proportional counter and its cabling may be located in the vacuum environment and the vacuum seal made at the preamplifier back plate. Application of

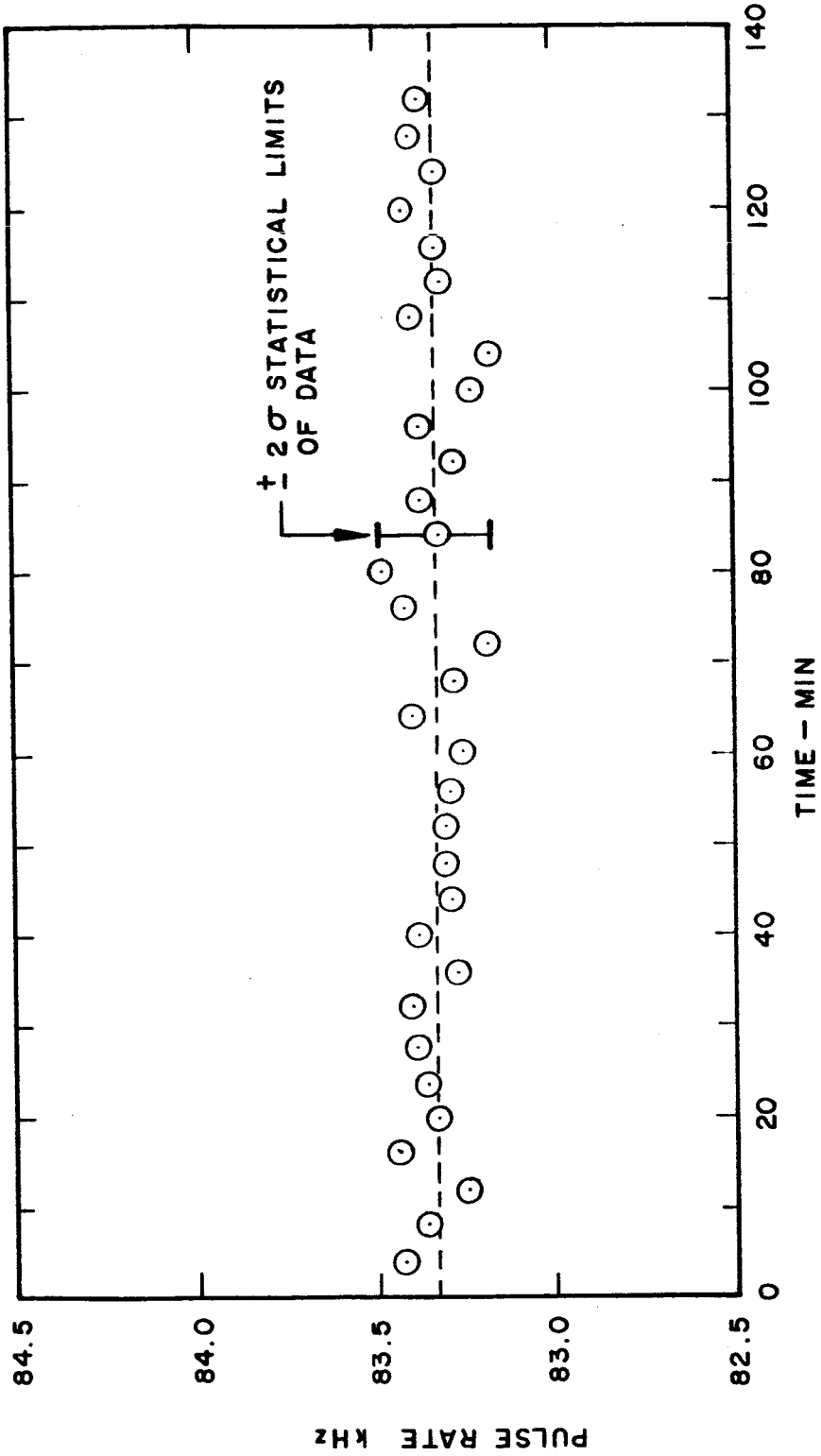

FIGURE 24 - Stability Data

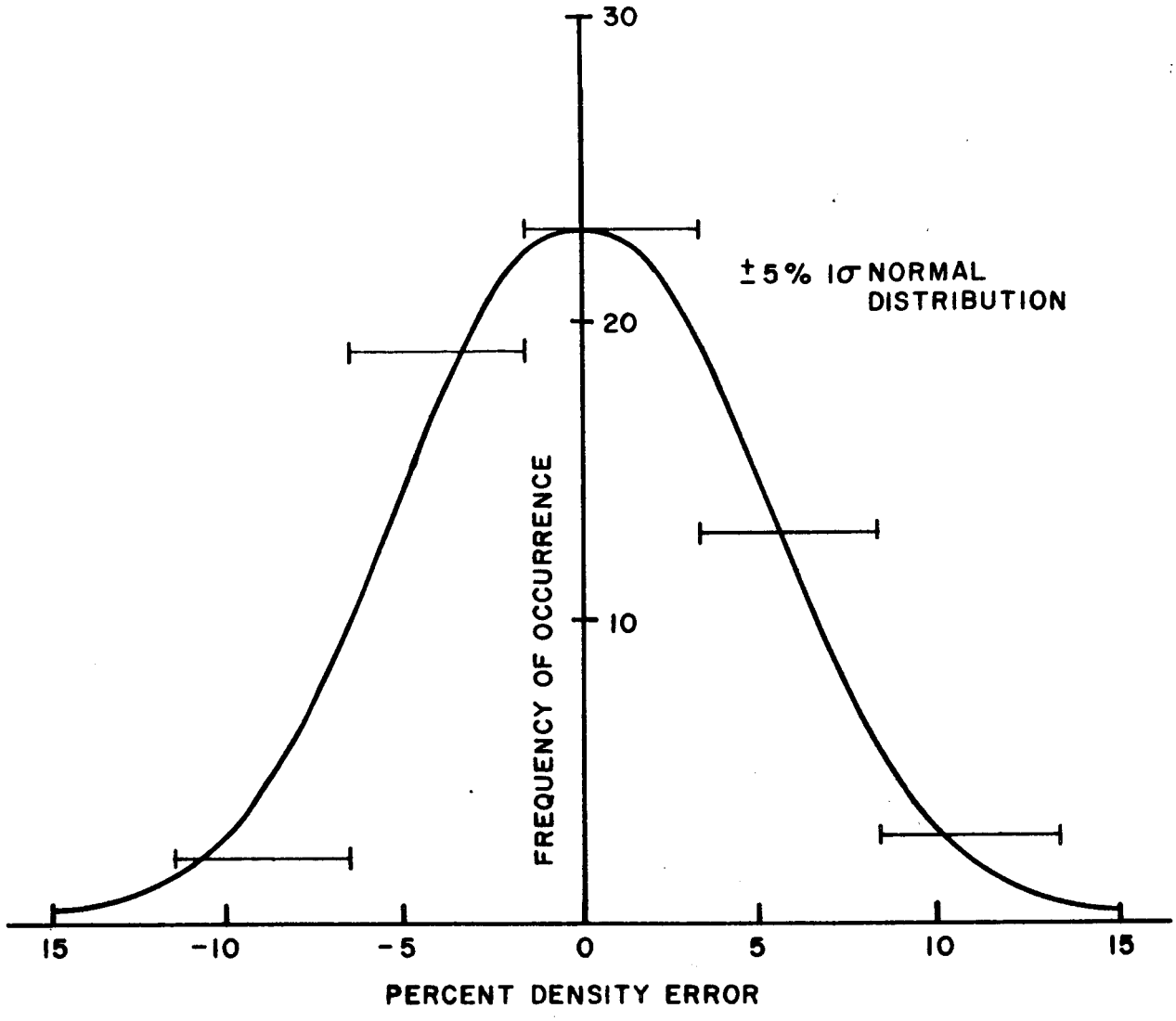

FIGURE 25 - Repeatability Distribution

silicone grease to the high voltage connections is recommended to prevent voltage arcing in the vacuum. Gas hoses connect the proportional counter chamber to the gas regulator and vent it to the atmosphere. The hose containing the capillary tube section is connected between the gas regulator and proportional counter tube. The gas regulator is adjusted to approximately 3 psig pressure, allowing a nominal gas flow through the counter tube. Before operation of the proportional counter tube, the gas mixture should be allowed to purge the tube for at least 30 minutes. For greatest stability, the tube should be purged for approximately 8 hours. The gas is normally left flowing continuously, eliminating the need for purge cycles. The main detector cable is connected from the console to the preamplifier.

The X-ray tube is mounted to an interface plate, making the vacuum seal to the X-ray tube face. Filament leads are connected through the protective cover. The high voltage cable is connected directly to the X-ray tube anode with its shield grounded to the interface plate. The blower is mounted to the interface plate, directing cooling air at the X-ray tube. Power for the blower is supplied from the operation console.

The path length is defined as the distance from the front surface of the X-ray tube face plate to the surface of the proportional counter tube window.

System Setting Adjustment

Recommended settings of the operation console are listed in table III. After a check of these settings, the following

TABLE III

RECOMMENDED CONTROL CONSOLE SETTINGS

CONTROL PANEL	
Time Constant Switch	See calibration chart
Operation Mode Switch	Off
REFERENCE POWER SUPPLY	
Range Switch	0-10 volts
Current Limit Potentiometer	Maximum
Voltage Adjustment Switch	See calibration chart
FILAMENT POWER SUPPLY	
Voltage Adjustment Potentiometer	0 volt
Current Limiter Adjust. Potentiometer	See operation sequence items 4, 5, and 6
PLATE VOLTAGE POWER SUPPLY	
Standby/Operate Switch	Standby
Voltage Adjustment Switch	1.500 kV
Polarity Switch	+
COUNTER	
Sensitivity Switch "A"	+1.5 volts
Slope Switch	+
Mode Switch	Sep.
Function Switch	Frequency A
Time Base Switch	1.0 second
Sample Rate Potentiometer	Minimum
DIGITAL RECORDER	
Record Switch	Off
DISCRIMINATOR	
Coarse Gain Switch	16
Fine Gain Potentiometer	0.875
Function Switch	E_L
ΔE Potentiometer	N/A
E_u Potentiometer	N/A
E_L Potentiometer	0.010
PROPORTIONAL COUNTER POWER SUPPLY	
High Voltage Switch	On
High Voltage Adjust. Potentiometer	0.730

operation sequence is recommended.

Operation Sequence

1. Set the Operation Mode switch in the Off position.
2. Turn all instrument On-Off switches in the On position.
3. Set the Operation Mode switch to Manual position.
4. Increase the filament power supply Voltage Adjust potentiometer until the filament current is approximately 2.0 amperes.
5. Adjust the filament power supply Current Limiter poteniometer to limit at approximately 2.0 amperes.
6. Set the Operation Mode switch to Offset Adjust position.
7. Adjust the Offset Adjust control (screwdriver adjustment) for a voltage output of zero volts ±0.005 volt at the amplifier output terminals.
8. Place the Time Constant switch to that position specified on the calibration setting table (Table II.) for the path length selected.
9. Set the Reference Voltage Adjust switch to that value specified on the calibration chart for the path length selected.
10. Set the Plate Voltage Control switch to 1.5 kV and the Standby/Operate switch to Standby.
11. Set the Operation Mode switch to Filament Warmup position.
12. When the plate voltage power supply lamp turns on, place the Standby/Operate switch to Operate.
13. Adjust the Plate Voltage Control switch to the value

specified on the calibration chart.

14. Set the Operation Mode switch to the Operate position.

15. Set the digital recorder Record Switch to On.

16. The System is now operating in its normal mode.

Collimator Alignment

The collimator is chosen for the particular X-ray path length selected, as defined on the calibration chart. The collimator is inserted in the collimator alignment fixture with the back end flush with the back face of the fixture. The fixture is then installed on the interface plate and alignment adjustment made via the adjusting bolts.

Alignment of the collimator is best accomplished by activating the X-ray tube and detector system and measuring the count rate obtained. The X-ray tube is then deactivated and the collimator again adjusted. Another count rate is taken and compared with the previous count rate. Adjustment and count rate measurement cycles are repeated until the highest count rate is obtained. A small shield, with a 0.635 cm diameter hole, centered in front of the proportional counter window, will greatly facilitate this alignment.

With the alignment completed, the system is ready for density measurement.

Overload Reset Cycle

If an accidental overload occurs, the X-ray tube plate voltage power supply will automatically turn off and the filament voltage will be reduced to zero. The following procedure is

applicable in this situation.

1. Place the plate voltage power supply Standby/Operate Switch to Standby.
2. Adjust the Plate Voltage Control switch to 1.5 kV.
3. Place the Operation Mode switch in the Filament Warmup position and check for proper setting of the Time Constant switch.
4. Repeat steps 13 to 16 of previous section, Operation Sequence.

SAFETY

Two safety considerations are important in the operation of the system. The first involves use of the high voltage equipment. Care should be exercised to avoid contact with the X-ray high voltage terminals. Some physical protection has been provided in the form of a partial housing over the X-ray tube such that with normal care no hazard exists.

The second consideration involves X-ray dosage. With the X-ray energies involved, 0-5 keV, the X-ray tube envelope absorbs all the flux except for the output beam. One mm of glass attenuates 5 keV X-rays by a factor of 1.62×10^{-29}. For 5 kV, 10 mA operation, the total X-ray power generated from equation 4 is

$$I_w = 1.4 \times 10^{-12} \times 10 \times 74 \times (5 \times 10^3)^2 = 0.0259 \text{ watts}$$

At the X-ray tube surface, 2 cm away from the target and

after attenuation by the glass envelope, the intensity is found to be

$$\frac{0.0259 \times 1.62 \times 10^{-29}}{4\pi(2)^2} = 8.35 \times 10^{-33} \text{ watts/cm}^2$$

This is equivalent to 8.35×10^{-26} ergs/cm^2-second. The range in tissue at which 95% of the energy is absorbed is 0.071 cm. Since 1 rad is equal to 100 ergs/gm of absorbed dose, the dose rate at the surface of the X-ray tube envelope is

$$D = \frac{8.35 \times 10^{-26} \text{ ergs}}{\text{cm}^2 - \text{sec}} \times \frac{1 \text{ rad-gm}}{100 \text{ ergs}} \times \frac{\text{cm}^3}{1 \text{ gm}} \times \frac{1}{.071 \text{ cm}} = 1.175 \times 10^{-26} \text{ rad/sec}$$

or converting units.

$$D = 4.22 \times 10^{-20} \frac{\text{millirad}}{\text{hour}}$$

(The ambient radiation level at the surface of the earth is about $0.008 \frac{\text{millirad}}{\text{hour}}$.)

At the X-ray tube window a 5 keV flux of 100,000 pulses per second in a 0.635 inch diameter beam has an intensity of

$$\frac{100{,}000 \text{ pulses}}{\text{sec}} \times \frac{5 \text{ keV}}{\text{pulse}} \times \frac{4}{(.635)^2 \pi \text{ cm}^2} \times \frac{1 \text{ erg}}{6.25 \times 10^8 \text{ keV}}$$

$$= 2.54 \times 10^{-3} \frac{\text{ergs}}{\text{cm}^2 - \text{sec}}$$

The dose rate at this intensity is

$$\frac{2.54 \times 10^{-3} \text{ ergs}}{\text{cm}^2 - \text{sec}} \times \frac{1 \text{ rad - gm}}{100 \text{ ergs}} \times \frac{\text{cm}^3}{1 \text{ gm}} \times \frac{1}{.071 \text{ cm}} \times \frac{3600 \text{ sec}}{\text{hr}}$$

$$= 1.29 \frac{\text{rad}}{\text{hr}}$$

This is a significant dose rate and direct exposure to any part of the body should be avoided.

CONCLUSIONS, RECOMMENDATIONS, AND APPLICATIONS

This program has resulted in the design and fabrication of a Soft X-ray Absorption-Mode Gas Density Measuring System which meets all of the stated requirements. The theoretical models generated at the inception of this work were verified. Second order effects, such as dose buildup and gas fluorescence, were found to be negligible. An unexpected dual output characteristic of the X-ray tube due to target contamination was found to improve system accuracy but at the expense of requiring a separate calibration curve for each X-ray path length.

The equipment fabricated was found to be highly reliable. At the time of this writing, the system has been operating for a total of approximately 400 hours, without a single failure.

The system is suitable for application to laboratory facilities where the X-ray tube source and proportional counter detector can be mounted on each side of the gas flow and the operating rate can be located near the test chamber. The knowledge and experience obtained in the development of this laboratory system provides a sound basis for development of similar gas density measurement systems of small size and weight applicable to measurements in unfriendly environments.

It is recommended that further study in the areas of X-ray tube target contamination, X-ray tube thin window fabrication, and collimator design would benefit the program and result in less severe accuracy requirements of associated equipment. This

would further improve system accuracy and increase the dynamic range of measurement. Methods of automatic computation can be developed to provide a direct readout of the measured density, eliminating the need for calibration charts.

GIANNINI CONTROLS CORPORATION
DUARTE, CALIFORNIA
18 July 1966

APPENDIX

X-RAY TUBE STABILIZATION LOOP ANALYSIS

The X-ray tube stabilization loop is illustrated in figure 26. The plate current, i_p, is accurately controlled by a precision voltage reference, V_r. The plate current passes through a 100 ohm precision resistor off of which is taken the feedback voltage, V_{fb}. The transfer characteristics of this feedback resistor, K_3, is

$$K_3 = 0.10 \text{ volts/milliampere}$$

This feedback voltage is negatively summed with the reference voltage to give the error signal, ε. The error signal is operated on by the transfer function $\frac{1}{\tau_1 s}$. The summation and transfer characteristics are generated by the operational amplifier network shown in figure 27. Removal of resistor R_2 provides lead to the loop, improving dynamic response.

K_1 is the control characteristic of the filament power supply. The transfer function K_1 is given by

$$K_1 = 1.0 \text{ volt/volt}$$

The transfer function of the X-ray tube is a single order lag and a non-linear gain.

$$\frac{i_p}{V_f} = \frac{K_2}{\tau_2 S + 1}$$

The lag τ_2 is about 2 seconds, caused by the filament warmup characteristics. The relation between plate current and filament voltage is shown in figure 28. The gain K_2 is shown at four values of plate current.

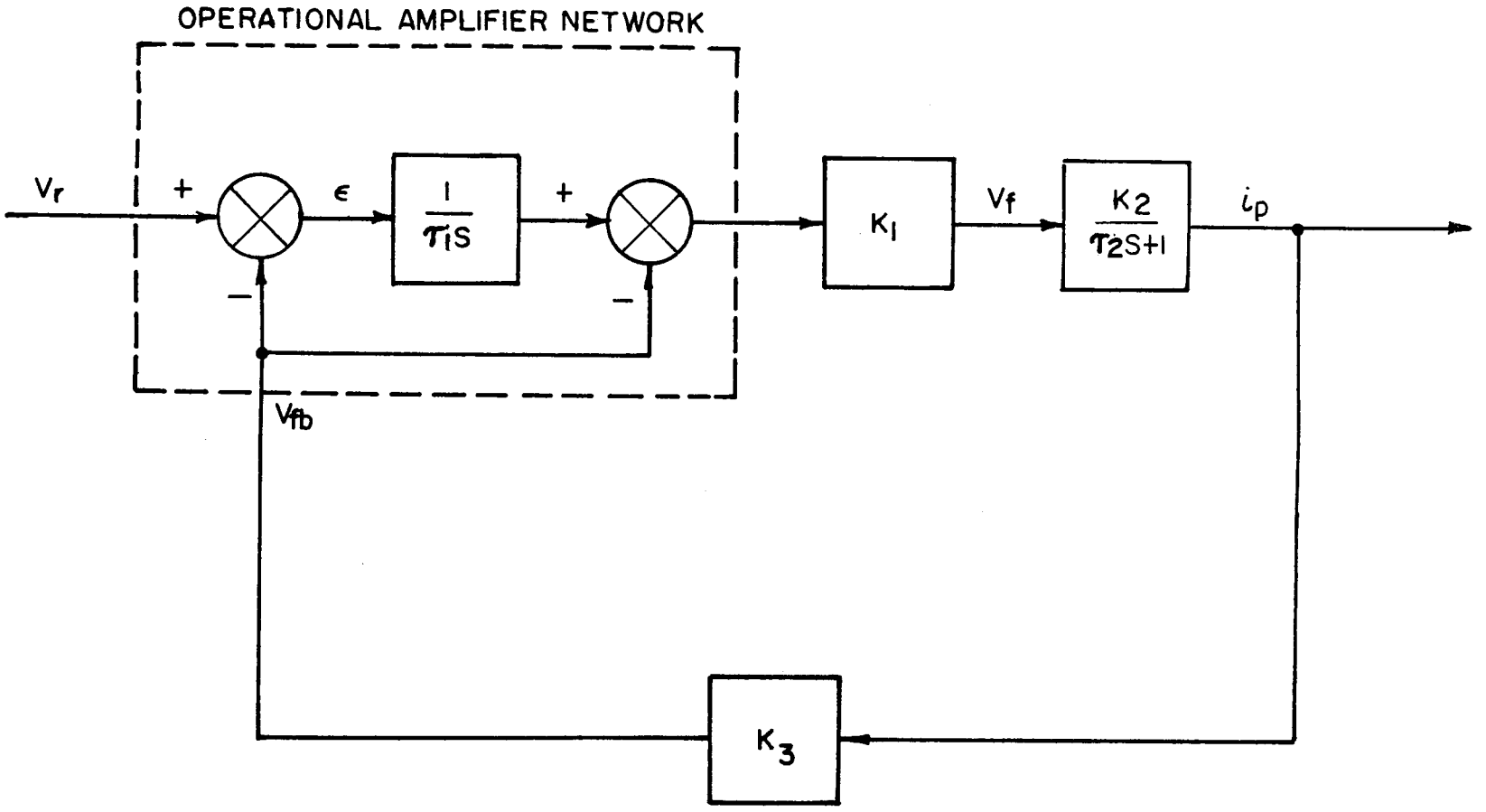

FIGURE 26 - X-ray Tube Stabilization Loop Diagram

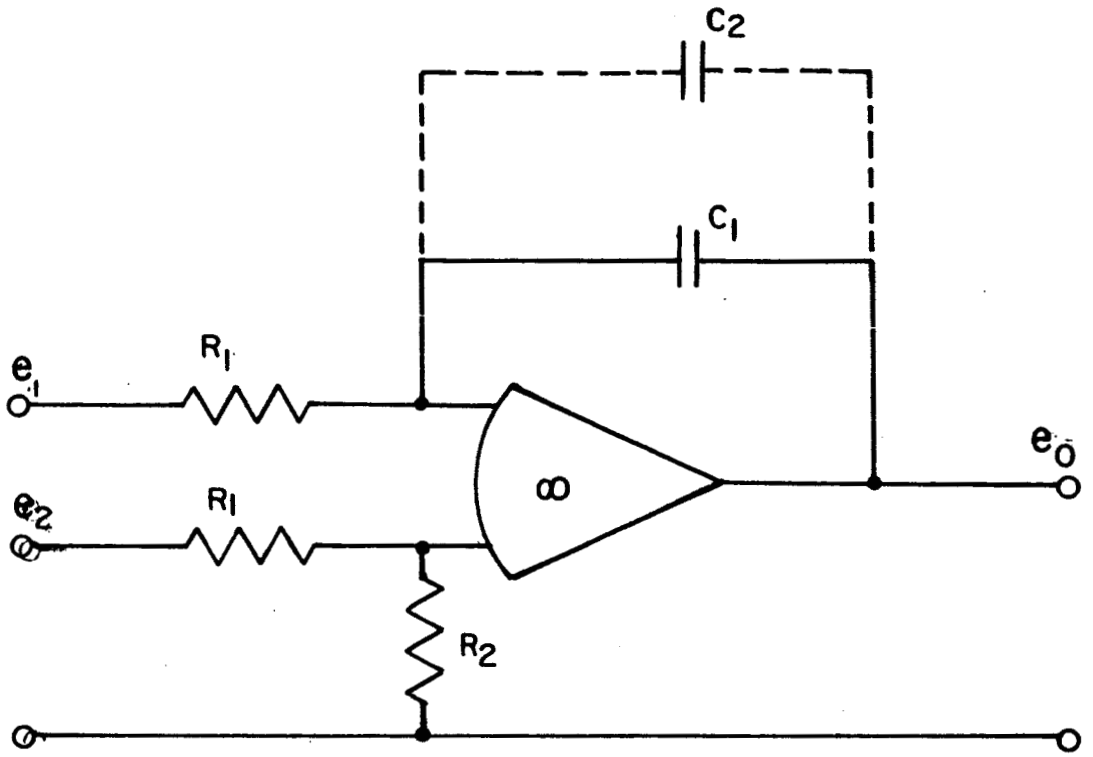

$$e_o = \frac{R_2}{R_1}\left(\frac{R_1 + \frac{1}{CS}}{R_1 + R_2}\right)E_2 - \frac{\frac{1}{CS}}{R_1}E_1$$

FOR $R_2 = \infty$

$$e_o = e_2 + \frac{1}{R_1 CS}\left(e_2 - e_1\right)$$

FIGURE 27 - Operational Amplifier Network

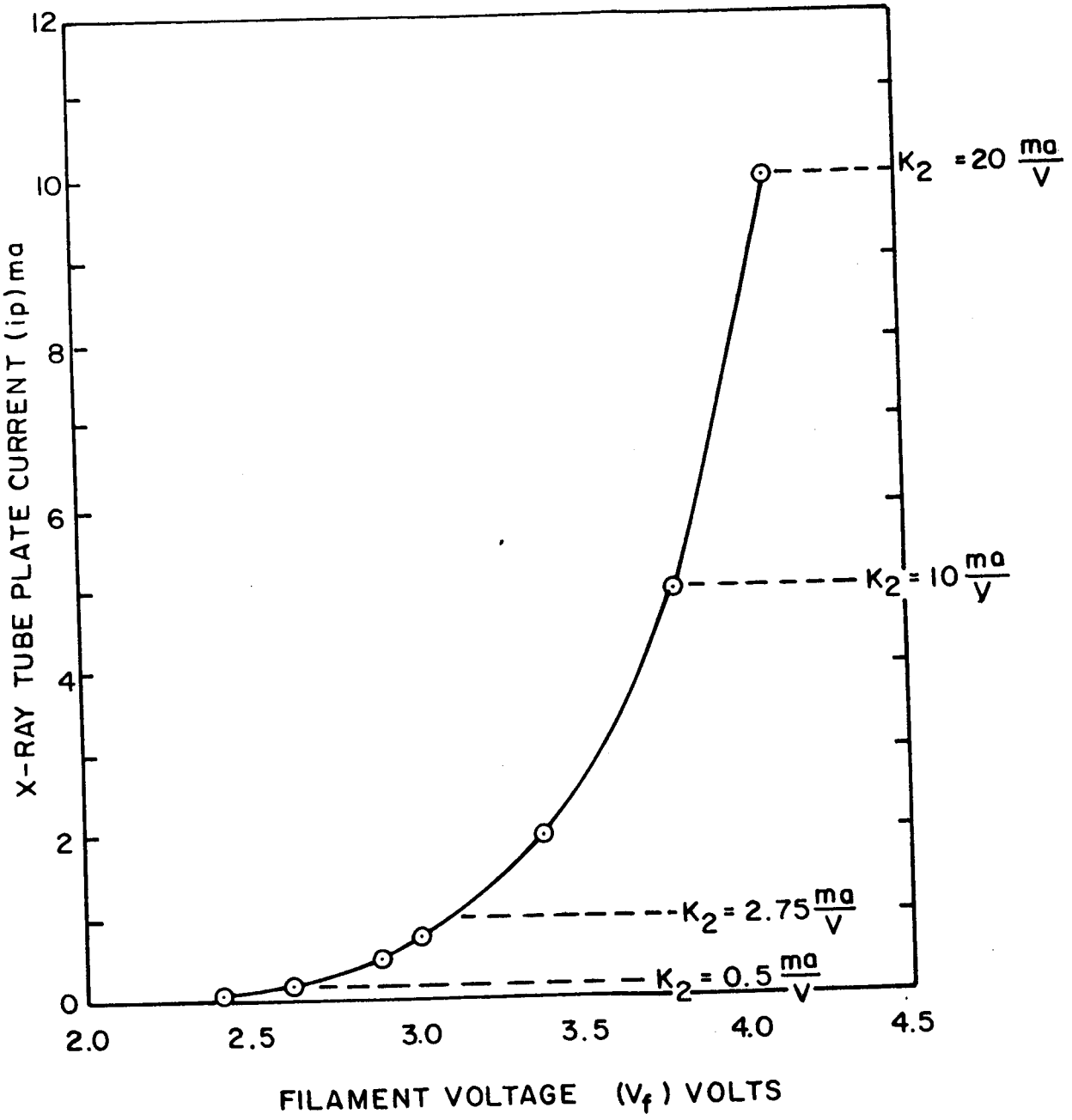

FIGURE 28 - X-ray Tube Gain Characteristics

Examination of figure 26 gives the system open loop transfer function G of

$$G = \frac{K_1 K_2 K_3}{\tau_1 s} \frac{\tau_1 s + 1}{\tau_2 s + 1}$$

The loop stability is examined on the root locus plot of figure 29 for two values of integrator capacitance, giving a high response and low response. The system response at the four plate currents is tabulated below.

	Plate Current i_p (ma)	Natural Frequency ω_n rad/sec	Damping Ratio ζ
High Response	0.1	0.8	0.33
	1.0	1.9	0.20
	5.0	3.7	0.20
	10.0	5.2	0.23
Low Response	0.1	0.35	0.75
	1.0	0.8	0.40
	5.0	1.5	0.35
	10.0	2.1	0.36

For plate current settings above 5 mA, the low response capacitance values are used. For settings below 5 mA, the high response setting is used, providing good response and damping for all conditions.

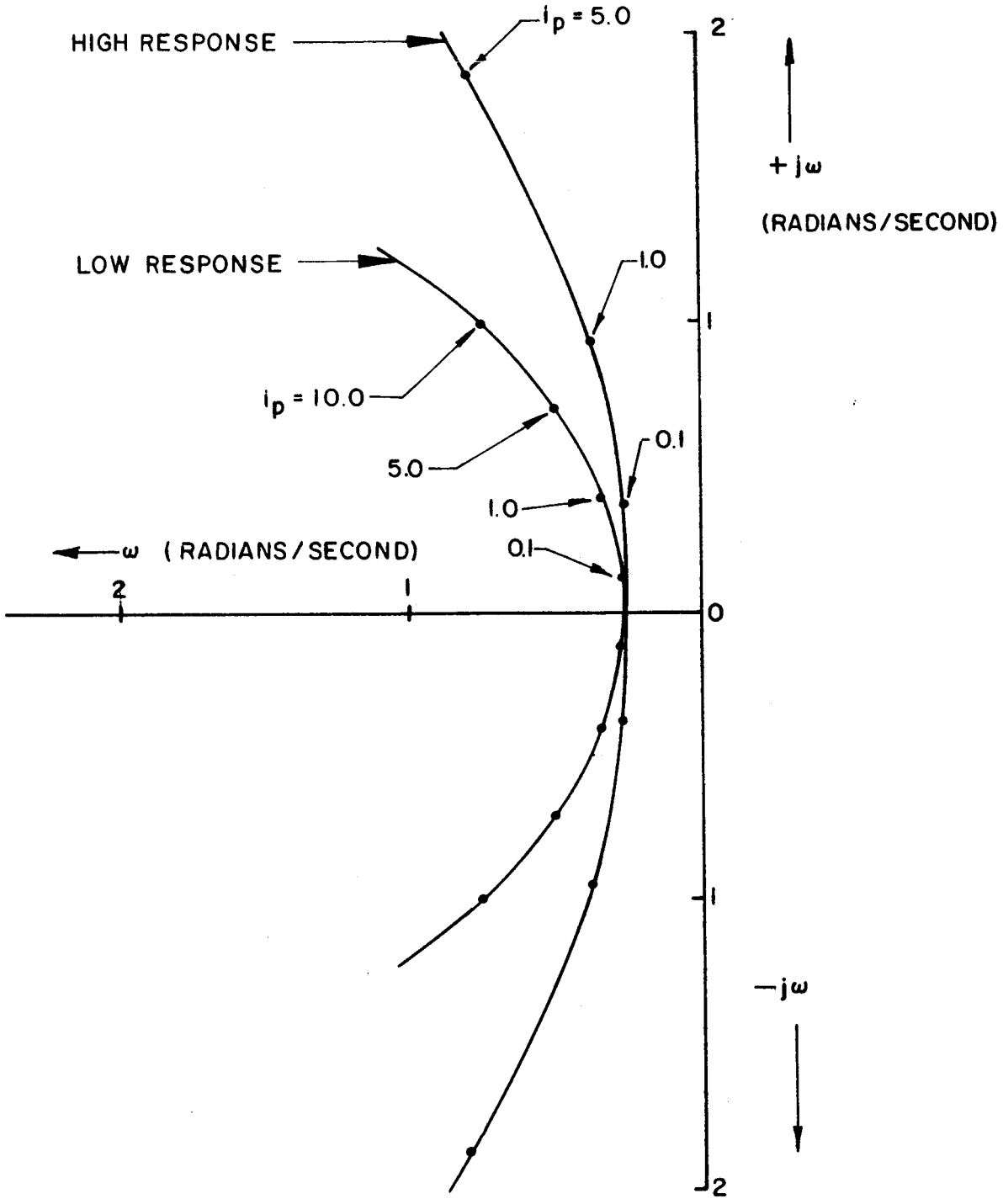

FIGURE 29 - Root Locus Showing Stability Characteristics

REFERENCES

1. Hine, Gerald J.; and Brownell, Gordon L.: Radiation Dosimetry. Academic Press, Inc. 1956, pp. 81.

2. Hodgman, Charles D., ed.: Handbook of Chemistry and Physics, Forty-second Edition, The Chemical Rubber Publishing Co., pp. 2662-2663.